Winter 1975

AN EXPERIMENTAL DETERMINATION OF THE LIFETIME OF THE TRIPLET-P(1) METASTABLE LEVEL OF CALCIUM AND MAGNESIUM

PAUL STEPHEN FURCINITTI

AN EXPERIMENTAL DETERMINATION OF THE LIFETIME OF THE $^3P_1$ METASTABLE LEVEL OF Ca AND Mg

by

PAUL S. FURCINITTI

B.S., Worcester Polytechnic Institute, 1971

M.S., University of New Hampshire, 1974

A THESIS

Submitted to the University of New Hampshire

In Partial Fulfillment of

The Requirements for the Degree of

Doctor of Philosophy

Graduate School

Department of Physics

December, 1975

This thesis has been examined and approved.

Thesis Director, L. C. Balling, Assoc. Prof. of Physics

John F. Dawson, Asst. Prof. of Physics

Richard Kaufmann, Prof. of Physics

Robert H. Lambert, Prof. of Physics

John J. Wright, Asst. Prof. of Physics

Mar. 24, 1975
Date

ACKNOWLEDGEMENTS

The author wishes to express his gratitude to his adviser, Dr. L. Christian Balling and also to Dr. John J. Wright for suggesting this investigation and for their enthusiastic participation in all facets of this work.

The author also wishes to thank: Mr. Gregory Rocco for writing the machine language program used by the PDP-LAB8/E computer to acquire and analyze the bulk of the experimental data obtained in this work; Ms. Susan Horner for typing various drafts of this thesis; and Mr. Daniel Gats and Ms. Janet Varney for preparing the illustrations appearing in this work.

A debt of gratitude is owed to my fellow graduate students, Bruce Bean, Jerome Hojnacki, Ezra and Sandy Mann, and John O'Shea for their continued encouragement and support throughout the entire course of my graduate work.

Finally, the author wishes to thank his parents for their unfailing support and encouragement in this as well as all his other endeavors.

This research was supported by the National Science Foundation and the Research Corporation.

TABLE OF CONTENTS

LIST OF TABLES

LIST OF ILLUSTRATIONS

ABSTRACT

AN EXPERIMENTAL DETERMINATION OF THE LIFETIME OF THE $^3P_1$ METASTABLE LEVEL OF Ca AND Mg

by

PAUL S. FURCINITTI

An experimental technique for determining the lifetime of the $^3P_1$ level of Group II atoms has been developed and tested. The lifetimes obtained by this method may be used to determine absolute oscillator strengths of the $^1S_0 \leftrightarrow {}^3P_1$ transition for the alkaline earth elements.

An experimental determination of the lifetime of the $^3P_1$ level of Ca and Mg was made using this technique. An intense pulse of radiation from a dye laser was used to selectively populate the $^3P_1$ level of these atoms. The absorption of light from a Ca or Mg radio frequency discharge lamp by atoms in the $^3P_2$, $^3P_1$, or $^3P_0$ level was monitored as a function of time. These measurements allowed the time dependence of the population of the $^3P_1$

level and hence its lifetime to be determined. The experimental values obtained in this investigation for the lifetime of the Ca and Mg $^3P_1$ level were 0.393 $\pm$ 0.040 and 4.54 $\pm$ 0.30 msec respectively.

CHAPTER I

INTRODUCTION

Accurate determinations of absolute transition probabilities and lifetimes of atomic and ionic excited states have applications in several fields of physics. Astrophysical applications of these quantities include determinations of the constituents of stellar atmospheres and of the chromosphere and corona of the Sun.[1] Accurate lifetime measurements are also of interest in experimental work concerning plasma diagnostics,[2-3] studies of line broadening,[3-4] and the investigation of populations in a discharge.[5]

In particular, accurate absolute transition probabilities for the spin-forbidden electric dipole transitions in Ca and Mg which give rise to the ($4s4p\ ^3P^0_1 \leftrightarrow 4s^2\ ^1S_0$) and ($3s3p\ ^3P^0_1 \leftrightarrow 3s^2\ ^1S_0$) intercombination lines would have several applications. Accurate lifetime determinations for these spin-forbidden transitions are of interest for the interpretation of radiative emissions from laboratory and astrophysical plasmas.[6-7] Also, a new absolute frequency standard proposed by Strumia[8] requires that the lifetimes of the Ca and Mg $^3P_1$ level be known accurately. Finally, accurate measurements of these lifetimes are also

required in order to test the validity of the assumptions and approximations made in theoretical calculations of these quantities.

Most of the experimental values for the lifetimes of the Ca and Mg $^3P_1$ levels have been obtained from relative oscillator strength measurements. Summaries of the theoretical and experimental values for the Ca and Mg $^3P_1$ metastable level lifetimes are presented in Tables 1 and 2. In the case of Mg there has been a long standing discrepancy between the values of the $^3P_1$ lifetime obtained by experimental measurements[21, 25-30] and theoretical calculations.[11, 14, 21-24] An inspection of Table 2 indicates that the experimental results have also been contradictory.

The purpose of this investigation was to obtain measurements of the Ca and Mg $^3P_1$ level lifetime from which absolute oscillator strengths for the $^1S_0 \leftrightarrow {}^3P_1$ transitions in Ca and Mg can be deduced. It was also hoped that the discrepancy between the theoretical and experimental values for the Mg $^3P_1$ lifetime would be resolved. An examination of Tables 1 and 2 shows that the lifetime values obtained in this work are in substantial agreement with the most recent theoretical values.

Usually the lifetimes of excited states which decay directly to the ground state are determined by fluorescence measurements.[31-33] However, Ca and Mg have three fine structure P levels (viz., the $^3P_2$, $^3P_1$ and $^3P_0$ levels). The populations of these levels are in thermal

TABLE 1

SUMMARY OF THEORETICAL AND EXPERIMENTAL VALUES FOR THE Ca $^3P_1$ METASTABLE LEVEL LIFETIME

AUTHOR	THEORY τ(msec)	EXPT τ(msec)
King and Van Vleck[9] (1939)	0.32	
Vainshtein and Poluektov[10] (1961)	0.33[a]	
Warner[11] (1968)	0.22	
Luc-Koenig[12] (1974)	0.34	
Victor[13] (1975)	0.34	
Prokofjew[14] (1928)		0.35[a]
Schuttevaer et al.[15] (1943)		0.08[b]
Olsen et al.[16] (1959)		0.53[c]
Ostrovskii and Penkin[17] (1961)		0.39[a]
Penkin[18] (1964)		0.44
NBS Tables[19] (1969) (weighted average)		0.37 $\pm$ 0.19
This Work[20]		0.393 $\pm$ 0.040

[a]Calculated or measured relative to Ca $^1S_0 \leftrightarrow {}^1P_1^0$ transition, normalized to 4227-Å line of NBS Tables.

[b]Measured relative to Ca $^3P_0 \leftrightarrow {}^3D_1$ transition, normalized to 6103-Å line of NBS Tables.

[c]Measured relative to Ca $^3P_0 \leftrightarrow {}^3S_1$ transition, normalized to 6103-Å line of NBS Tables.

TABLE 2

SUMMARY OF THEORETICAL AND EXPERIMENTAL VALUES FOR THE Mg $^3P_1$ METASTABLE LEVEL LIFETIME

AUTHOR	THEORY τ(msec)	EXPT τ(msec)
Prokofjew[14] (1928)	5.0	
Frayne[21] (1929)	4.0	
Rubenstein[22] (1940)	3.8	
Garstang[23] (1962)	4.2	
Warner[11] (1968)	5.2	
Laughlin and Victor[24] (1974)	4.6	
Frayne[21] (1929)		4.0
Boldt[25] (1958)		1.9 ± 0.4
NBS Tables[26] (1969) (weighted average)		2.3 ± 1.2
Wright et al.[27] (1974)		2.2 ± 0.2
Strumia et al.[28] (1974)		1.8 ± 0.2
Mitchell[29] (1975)		3.8 ± 1.2[a]
This Work[30]		4.54 ± 0.30

[a] Measured and normalized relative to Mg $^1S_0 \leftrightarrow {}^1P_1^0$ transition.

equilibrium due to thermal mixing collisions in the presence of an inert buffer gas. Furthermore, the transitions $^1S_0 \leftrightarrow {}^3P_2$ and $^1S_0 \leftrightarrow {}^3P_0$ are forbidden by the selection rules for electric and magnetic dipole as well as electric quadrupole radiation. This means that the atoms in the ^3P levels can only decay back to the ground state via the $^3P_1 \leftrightarrow {}^1S_0$ transition. These effects combine to produce an apparent lengthening of the observed $^3P_1$ lifetime. From these facts it should be clear that measurements of the fluorescence from the $^3P_1$ level alone would in themselves be insufficient to determine the $^3P_1$ lifetime, if the degree of mixing of the populations of the ^3P levels were unknown. Simultaneous measurements should be made to determine the degree of mixing of the populations of the ^3P levels. This would require some sort of absorption monitoring of the $^3P_2$ and $^3P_0$ populations since fluorescence cannot be observed from these levels.

The experimental method employed in this investigation to acquire the bulk of the experimental data for the determination of the Ca and Mg $^3P_1$ metastable level lifetime will now be described. Radiation from a pulsed dye laser was used to excite Ca or Mg atoms from their ground state, $^1S_0$, to the $^3P_1$ excited state. Light from a Ca or Mg radio frequency discharge lamp excited atoms in the $^3P_2$, $^3P_1$, and $^3P_0$ levels to higher excited levels by the process of absorption. In Chapter II the amount of absorption will be shown to be proportional to the populations

of the $^3P_2$, $^3P_1$ and $^3P_0$ levels. This being the case, measurements of the absorption of the lamp light as a function of time would yield measurements of the population of the $^3P_1$ level as a function of time. The absorption signal decayed as a function of time as the atoms in the $^3P_1$ level returned to the ground state. The lifetime of the $^3P_1$ level was determined by ascertaining the decay constant of the absorption signal by a least squares fitting process. The systematic errors inherent in this lifetime measurement procedure will be discussed in Chapter IV.

The absorption method for lifetime determinations used in this investigation was suggested by a recent paper by McIlrath.[34] This paper described an experiment which proved the feasibility of populating the $^3P_1$ metastable level of Ca by tunable dye laser excitation and then performing absorption measurements on the metastable atoms so produced. A later paper by McIlrath and Carlsten[35] discusses the theoretical considerations involved in such an experiment. An earlier experiment performed by Asada et al.[36] to study the population of metastable Hg atoms in N_2 also employed absorption monitoring techniques. However, in the latter experiment convential spectroscopic light sources were used.

The dye laser excitation technique was employed by Wright, Dawson and Balling[27] to determine the lifetime of the Mg $^3P_1$ level. Their results, however, did not

remove the discrepancy between the theoretical and experimental values for this lifetime alluded to previously. It is now believed that a large systematic error was introduced into their results by the presence of contaminants in their absorption cell.[30] These contaminants participated in quenching collisions with the metastable $^3P_1$ atoms.

The overall experimental design for this investigation first called for a measurement of the Ca $^3P_1$ lifetime. This lifetime is reasonably well known from other experimental and theoretical work.[9-20] Also, the Ca $^3P_1$ lifetime is a factor of 10 times shorter than that of Mg making it less susceptible to quenching effects. Agreement between the value obtained for the Ca $^3P_1$ lifetime by the techniques used in this work and the values obtained in other work would rule out the presence of any large sources of systematic error in the proposed experimental method. The successful completion of the above test would then be followed by a remeasurement of the Mg $^3P_1$ lifetime by the absorption technique. As a final test the Mg $^3P_1$ lifetime would also be measured in fluorescence.

In the following chapter the theoretical considerations necessary to understand the experiment will be described. The third chapter will be concerned with the experimental arrangement, apparatus and procedure. A presentation of the experimental data and results will be made in the fourth chapter. The fifth and final chapter will

present the conclusions deduced from this investigation along with suggestions for further study.

CHAPTER II

THEORY

In this chapter two topics will be discussed. They are the theory of $^3P_1 \leftrightarrow {}^1S_0$ spin-forbidden electric dipole transitions and the theory of absorption measurements of the lifetime of these transitions. The first section of this chapter will explain the nature and reasons for the occurrence of spin-forbidden transitions; this will involve a look at the configuration mixing caused by the spin-orbit interaction. The second section will discuss the theory of absorption measurements as they relate to the lifetime determinations made in this investigation. This will require an examination of the general expression for the absorption of radiation by an atomic gas. The absorption will be shown to be a function of the population of the ^3P levels (viz., the $^3P_2$, $^3P_1$ and $^3P_0$ levels). The absorption will also be shown to depend on the intensity and lineshape of the light emitted by the light source as well as the absorption coefficient of a gas of Ca or Mg atoms. The proper functional form for each of these quantities will be discussed. Particular attention will be accorded to the expression for the population of the ^3P levels since this expression involves the lifetime of the $^3P_1$ level. The

final portion of this chapter will discuss the functional form of the absorption signal when radiation is absorbed by Ca or Mg atoms in the ^3P levels. The absorption signal will be seen to be a function of the expressions derived for the populations of the ^3P levels, the absorption coefficient of the Ca or Mg atoms, and the emission line-shape of the radio frequency discharge lamp.

A. Spin-Forbidden Transitions

The purpose of this investigation was to experimentally determine the Ca and Mg $^3P_1$ level lifetimes corresponding to the intercombination transitions $4s4p\ ^3P_1^0 \leftrightarrow 4s^2\ ^1S_0$ and $3s3p\ ^3P_1^0 \leftrightarrow 3s^2\ ^1S_0$. These transitions are spin-forbidden electric dipole transitions. In the usual electric dipole radiation approximation transitions between singlet and triplet levels are not allowed. This selection rule is due to the fact that the electric dipole operator is independent of spin. Therefore, the only transitions which may occur are those for which the matrix element of the electric dipole operator is taken between two triplet or two singlet wavefunctions (i.e., $\Delta S = 0$). The transitions of interest in this investigation involve a change of spin, $\Delta S = 1$. Therefore, these transitions may be said to be spin-forbidden. However, the selection rule, $\Delta S = 0$, is only approximately true. In atoms with two valence electrons, the spin-orbit interaction mixes levels of different multiplicity allowing

spin-forbidden electric dipole transitions to occur.[24, 37-39] For example, in the case of Be I, a calculation by Nussbaum[39] shows that the spin-orbit interaction mixes $^1P_1^0$ levels with a $^3P_1^0$ level and $^3P_0$ levels with a $^1S_0$ level. This mixing produces a wavefunction for the $^3P_1$ level which may be written in the $|LSJM_J\rangle$ representation as[24]

$$|\Psi_i 1 M_{J_i}\rangle = (1-a^2)^{-1/2}\{|^3P\,1\,M_{J_i}\rangle + a\,|^1P\,1\,M_{J_i}\rangle\} \qquad (1).$$

The normalized wavefunction for the $^1S_0$ level may be written as

$$|\Psi_f 0 M_{J_f}\rangle = (1-b^2)^{-1/2}\{|^1S_0\,0\,M_{J_f}\rangle + b\,|^3P\,0\,M_{J_f}\rangle\} \qquad (2).$$

The constants a and b are given by

$$a = \frac{\langle ^1P1M_{J_i}|H_{S.O.}|^3P1M_{J_i}\rangle}{E^0(^3P_1) - E^0(^1P_1)} \qquad (3),$$

and

$$b = \frac{\langle ^3P0M_{J_f}|H_{S.O.}|^1S0M_{J_f}\rangle}{E^0(^1S_0) - E^0(^3P_0)} \qquad (4),$$

in which $H_{S.O.}$ is the spin-orbit portion of the Hamiltonian. The quantities $E^0(^3P_1)$, $E^0(^1P_1)$, $E^0(^1S_0)$ and $E^0(^3P_0)$ are the respective energy values of the $^3P_1$, $^1P_1$, $^1S_0$ and $^3P_0$ energy levels in the absence of the spin-orbit interaction. When the matrix element of the electric dipole operator is taken between the wavefunctions $|\Psi_i 1 M_{J_i}\rangle$ and $|\Psi_f 0 M_{J_f}\rangle$ its

value is seen to be non-zero. Therefore, the inter-multiplet $^3P_1 \leftrightarrow {}^1S_0$ electric dipole transition is allowed. This same formalism can be used to explain the $^3P_1 \leftrightarrow {}^1S_0$ transitions observed in Ca and Mg in terms of non-relativistic quantum mechanics. The lifetimes of these transitions are on the order of 10^{-4} and 10^{-3} seconds for Ca and Mg respectively, versus 10^{-8} seconds for the lifetime of a regular allowed electric dipole transition. A paper by Luc-Koenig[12] discusses the point that these spin-forbidden transitions are allowed in a relativistic quantum mechanical treatment of electric dipole radiation.

B. Absorption Measurements of Lifetimes

As stated in chapter I the lifetime of the Ca and Mg $^3P_1$ level was measured by monitoring the absorption of light by Ca and Mg atoms in the $^3P_2$, $^3P_1$ or $^3P_0$ levels. A measurement of the light absorbed as a function of time is proportional to a measurement of the population of the $^3P_1$ level as a function of time. As a concrete example of how such a measurement would be performed, consider a radio frequency discharge lamp which produces light of the wavelength corresponding to the Mg $^3P_2 \leftrightarrow {}^3S_1$ transition. The light from this lamp is incident on a cell containing an atomic vapor of Mg. Only a negligible fraction of the Mg atoms are initially in the $^3P_2$ excited level due to the low amount of thermal energy present. Therefore, almost all of the $^3P_2 \leftrightarrow {}^3S_1$ lamp light is initially transmitted

through the absorption cell. Let this transmitted light intensity be denoted by I_0. At some instant of time, t = 0, a laser is fired. The laser populates the Mg $^3P_1$ level. This laser pulse lasts for only 1 μsec. This time is negligible in comparison to the time during which measurements are made (i.e., $\sim 10^{-3}$ sec). As stated in Chapter I, thermal mixing of the populations of the $^3P_2$, $^3P_1$ and $^3P_0$ levels occurs. Thus, the $^3P_2$ level becomes populated when the $^3P_1$ level is populated. The lamp light corresponding to the transition $^3P_2 \leftrightarrow {}^3S_1$ can then be absorbed by the atoms in the $^3P_2$ level. The lamp light intensity that is transmitted through the absorption cell drops sharply as the absorption takes on its maximum value. As atoms in the $^3P_1$ level return to the ground state the population of the $^3P_2$ level also decreases since the two levels are in thermal equilibrium. (Recall that the transition $^3P_2 \leftrightarrow {}^1S_0$ is forbidden). The decay of metastable $^3P_1$ atoms causes the intensity transmitted through the absorption cell to increase and the absorption to decrease. Thus, by measuring the amount of light absorbed by atoms undergoing the transition $^3P_2 \leftrightarrow {}^3S_1$ as a function of time, the time dependence of the population of the $^3P_1$ level can also be measured. This was the method used in this experiment to measure the lifetime of the $^3P_1$ level of Ca and Mg. This process is graphically represented in Figure 1. These arguments will be placed on a more quantitative basis in the remainder of this chapter. The discussion will begin with a description

FIGURE 1

Graph of lamp intensity transmitted through absorption cell versus time. Prior to the population of the $^3P_1$ level by the laser, the intensity transmitted through the cell is a constant, I_0. When the laser is fired the lamp intensity transmitted through the cell drops sharply as the atoms in the ^3P levels absorb light, and increases exponentially as the atoms in the $^3P_1$ level return to the ground state.

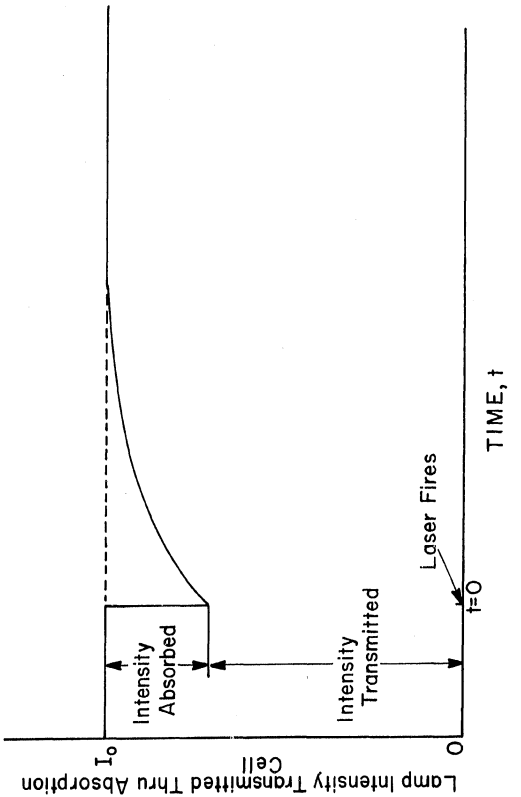

of absorption by an atomic gas. This will explicitly show how the absorption is related to the population of the absorbing level.

1. Absorption of Radiation by an Atomic Gas

The absorption of radiation by an atomic gas is treated in detail in a book by Mitchell and Zemansky[40] and also in a book by Loudon.[41] The "absorption", A, is defined as[42]

$$A = 1 - \frac{\text{transmitted radiation}}{\text{incident radiation}} \qquad (5).$$

From Figure 1 the magnitude of the absorption signal is seen to be equal to the incident radiation intensity, I_0, times the absorption, A. Let the frequency distribution of the light intensity emitted by a radio frequency discharge lamp be denoted by I_ν. Let the absorption coefficient of an atomic gas of Ca or Mg atoms be given by k_ν and let the thickness of the absorbing layer be given by ℓ. The absorption, A, may then be written as[43]

$$A = 1 - \frac{\int_{-\infty}^{\infty} I_\nu \exp(-k_\nu \ell)\, d\nu}{\int_{-\infty}^{\infty} I_\nu \, d\nu} \qquad (6).$$

The absorption coefficient, k_ν, may be defined in general as

$$k_\nu = \frac{N B_{12} h\nu F(\nu)}{c\eta V} \qquad (7).$$

In the above expression

N = the population of an excited atomic level. The atoms in this level may absorb the incident radiation produced by a radio frequency discharge lamp.

$F(\nu)d\nu$ = the probability that an atom will make a transition by the emission or absorption of a photon having a frequency between ν and $\nu + d\nu$. The function, $F(\nu)$, is also called the absorption or emission lineshape function.

B_{12} = the probability per unit energy density that an atom in the initial state, $|1\rangle$, will absorb a photon of frequency, ν_{12}, and be excited to a higher energy state, $|2\rangle$.

$h\nu/V$ = the energy per unit volume or energy density

c = the speed of light

η = the index of refraction of the gas of atoms ($\eta \simeq 1$ for a dilute atomic gas).

The absorption coefficient, k_ν, may also be written as

$$k_\nu = k_0 F(\nu) \qquad (8),$$

where

$$k_0 = \frac{N B_{12} h\nu}{c\eta V} \qquad (9).$$

It can be seen from the above expressions that the absorption coefficient and hence the absorption depends on the population, N, of atoms in an excited state that may absorb radiation. The absorption, A, is also seen to depend on the frequency distribution of the incident radiation from

the radio frequency discharge lamp, I_ν, as well as the absorption lineshape function, $F(\nu)$. The next three sections of this chapter will be devoted to a discussion of the proper functional form for N, $F(\nu)$ and I_ν. It will be shown that the predominant frequency dependence of k_ν arises from the factor $F(\nu)$ and not from the factor of ν in equation (7). Therefore, ν is usually considered to be the resonant frequency, ν_{12}, between the two levels of interest. This being the case, all of the other factors in k_ν except for N and $F(\nu)$ are considered to be known constants. It will also be shown that the population of the excited state, N, may be altered because of thermal mixing collisions between the atoms in the $^3P_2$, $^3P_1$ and $^3P_0$ levels. The problem of population alteration by absorption out of the $^3P_2$, $^3P_1$ and $^3P_0$ levels was investigated and was found to have had no effect on the observed lifetime. This phenomenon will be discussed in Appendix I.

2. Alteration of the $^3P_1$ Population and Lifetime by Thermal Mixing

As mentioned in Chapter I the observed lifetime, Γ, of the $^3P_1$ level is longer than the actual lifetime, τ. This is because there are three fine structure levels in the ^3P system which must be taken into account in lifetime determinations. These levels are the $^3P_2$, $^3P_1$ and $^3P_0$ levels. Let the fine structure energy level separations be given by ΔE_{20}, ΔE_{21} and ΔE_{10},

where

$$\Delta E_{20} = E(^3P_2) - E(^3P_0) \quad (10),$$

$$\Delta E_{21} = E(^3P_2) - E(^3P_1) \quad (11)$$

and

$$\Delta E_{10} = E(^3P_1) - E(^3P_0) \quad (12).$$

In the above equations $E(^3P_2)$, $E(^3P_1)$ and $E(^3P_0)$ are the energy values of the $^3P_2$, $^3P_1$ and $^3P_0$ fine structure levels. These energy level separations as well as the thermal energy present (i.e., 3/2 kT) during experimental determinations of lifetime values are listed in Table 3.

TABLE 3

FINE STRUCTURE ENERGY LEVEL SEPARATIONS AND THERMAL ENERGY PRESENT IN CM^{-1}

	Ca	Mg
ΔE_{20}	158	61
ΔE_{21}	106	41
ΔE_{10}	52	20
3/2 kT	886	834

In the Ca experiments $T \simeq 850^{\circ}K$ during experimental runs to determine the $^3P_1$ lifetime while in the Mg experiments $T \simeq 800^{\circ}K$. It can be seen from this table that the thermal energy present during investigations of the lifetime was greater than the fine structure energy level separations.

If the system was in thermal equilibrium the populations of the three levels would have been altered by mixing collisions between the atoms of this system and an inert buffer gas. Experiments were performed as a part of this investigation which indicated that the populations of the $^3P_2$, $^3P_1$ and $^3P_0$ levels were in thermal equilibrium for the Ca and Mg measurements. The data and results of these studies will be presented in Chapter IV. For this same system in Ca, McIlrath and Carlsten[35] have determined the mixing time to be less than 40 nsec with 10 Torr of He buffer gas in the absorption cell. This mixing time is much less than the 1 μsec duration of the laser pulse. The mixing affects the observed decay rate because an excited atoms spends only part of its time in the $^3P_1$ metastable level.

If N_1 is the total population of the ^3P system composed of the $^3P_2$, $^3P_1$ and $^3P_0$ levels than N_1 may be written as

$$N_1 = n_0 + n_1 + n_2 \tag{13}$$

in which n_0, n_1 and n_2 are the respective populations of the $^3P_0$, $^3P_1$ and $^3P_2$ levels. If the system is in thermal equilibrium, then[45]

$$n_2/n_1 = (g_2/g_1)\exp(-\Delta E_{21}/kT) \tag{14},$$

$$n_1/n_0 = (g_1/g_0)\exp(-\Delta E_{10}/kT) \tag{15}$$

and

$$n_2/n_0 = (g_2/g_0)\exp(-\Delta E_{20}/kT) \quad (16),$$

where g_2, g_1 and g_0 have the respective values of 5, 3 and 1 corresponding to the statistical weights of the $^3P_2$, $^3P_1$ and $^3P_0$ levels. In the above expressions k is Boltzman's constant, T is the absolute temperature and the fine structure energy separations are once again denoted by ΔE_{20}, ΔE_{21} and ΔE_{10}. The populations of the ^3P levels, n_0, n_1 and n_2, may be written as

$$n_0 = \alpha N_1 \quad (17),$$

$$n_1 = \beta N_1 \quad (18)$$

and

$$n_2 = \gamma N_1 \quad (19).$$

These equations imply that

$$1/\alpha = N_1/n_0 \quad (20),$$

$$1/\beta = N_1/n_1 \quad (21)$$

and

$$1/\gamma = N_1/n_2 \quad (22).$$

Equation (13) allows these last three equations to be written as

$$1/\alpha = (n_0 + n_1 + n_2)/n_0 = 1 + n_1/n_0 + n_2/n_0 \quad (23),$$

$$1/\beta = (n_0 + n_1 + n_2)/n_1 = 1 + n_0/n_1 + n_2/n_1 \quad (24)$$

and

$$1/\gamma = (n_0 + n_1 + n_2)/n_2 = 1 + n_0/n_2 + n_1/n_2 \quad (25).$$

The substitution of equations (14), (15) and (16) into equations (23), (24) and (25) allow α, β and γ to be expressed as follows:

$$\alpha = 1/\{1 + (g_1/g_0)\exp(-\Delta E_{10}/kT) + (g_2/g_0)\exp(-\Delta E_{20}/kT)\} \quad (26);$$

$$\beta = 1/\{1 + (g_0/g_1)\exp(+\Delta E_{10}/kT) + (g_2/g_1)\exp(-\Delta E_{21}/kT)\} \quad (27);$$

and

$$\gamma = 1/\{1 + (g_0/g_2)\exp(+\Delta E_{20}/kT) + (g_1/g_2)\exp(+\Delta E_{21}/kT)\} \quad (28).$$

Graphs of α, β and γ for Ca and Mg versus the absolute temperature are shown in Figures 2 and 3.

The $^3P_2 \leftrightarrow {}^1S_0$ and $^3P_0 \leftrightarrow {}^1S_0$ transitions are forbidden by the rigorous selection rules for electric and magnetic dipole as well as electric quadrupole radiation. Thus atoms in the ^3P system can only decay to the ground state via the $^3P_1 \leftrightarrow {}^1S_0$ transition. If A_{10} ($= 1/\tau$) is the transition rate for the $^3P_1 \leftrightarrow {}^1S_0$ transition then the time rate of change of the population of the ^3P system is given by

FIGURE 2

Population of the Ca $^3P_2$, $^3P_1$ and $^3P_0$ levels relative to the population of the ^3P system.

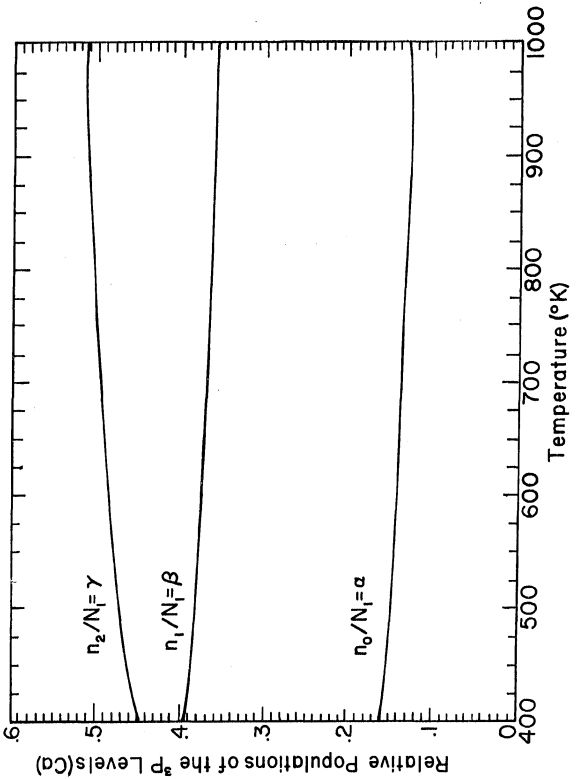

FIGURE 3

Population of the Mg $^3P_2$, $^3P_1$ and $^3P_0$ levels relative to the population of the ^3P system.

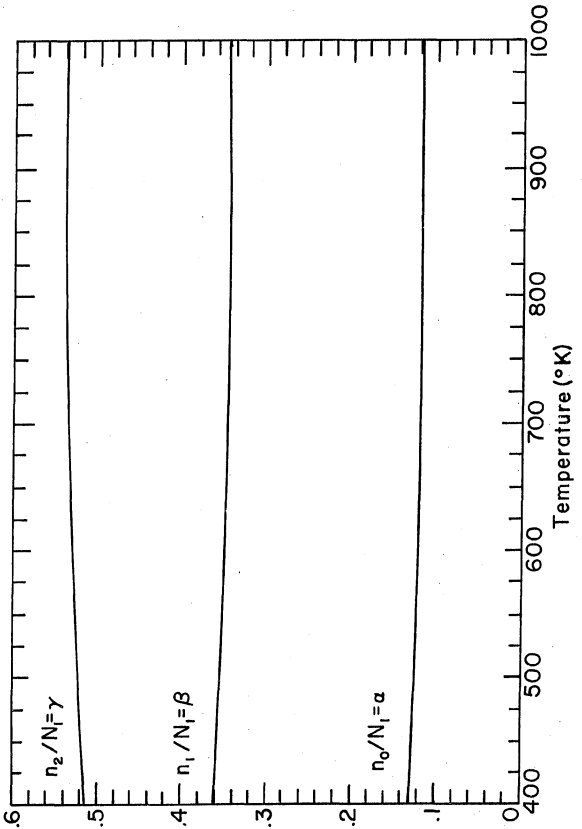

$$dN_1/dt = -A_{10} n_1 = -A_{10} \beta N_1 \tag{29}$$

or

$$N_1(t) = N_1(0) \exp(-A_{10} \beta t) = N_1(0) \exp(-t/\Gamma) \tag{30}$$

in which $N_1(0)$ is the population of the ^3P system at the instant that the dye laser is turned off and Γ is the observed lifetime of the $^3P_1$ level. (Recall that atoms in the ^3P system can only decay to the ground state via the $^3P_1 \leftrightarrow {}^1S_0$ transition).

Since

$$A_{10} \beta = \beta/\tau = 1/\Gamma \tag{31}$$

then

$$\tau = \beta \Gamma \tag{32},$$

where τ is the natural lifetime of the $^3P_1$ level and β is the fraction of the number of atoms in the ^3P system actually in the $^3P_1$ level. Since β is less than 1, the observed lifetime, Γ, is longer than the natural lifetime. Calculations to determine β from equation (27) for the range of temperatures in which data was taken yield values of β equal to 0.36 for Ca and 0.34 for Mg. These values are constant to within 1% in these temperature ranges. Thus, it has been shown that thermal mixing collisions alter the observed lifetime of the atoms in the $^3P_1$ level.

3. Phenomena Affecting the Absorption Coefficient

As alluded to in section B.1 of this chapter, an atom does not emit or absorb radiation at a single discrete frequency but can emit or absorb radiation over a range of frequencies. The probability, $F(\nu)d\nu$, that an atom will make a transition by the emission or absorption of a photon having a frequency between ν and $\nu + d\nu$ is affected by various phenomena. The absorption coefficient, k_ν, is a function of this probability as shown in the preceding section. The various processes which affect the probability are often said to broaden the absorption line.

They are:

1) Natural broadening due to the finite lifetime of an excited state;

2) Doppler broadening due to the motion of the atoms;

3) Lorentz broadening due to collisions with foreign gas atoms or molecules; and

4) Holtsmark broadening due to collisions with other absorbing atoms of the same kind.

One may determine the relative importance of the various line broadening mechanisms by calculating the full width at half maximum, $\Delta\nu$, of the absorption profile due to each broadening mechanism. In the case of natural line broadening $\Delta\nu_N$ is given by[46]

$$\Delta\nu_N = 1/(2\pi\tau_{21}) \qquad (33),$$

where τ_{21} is the natural lifetime of the transition involved in the absorption process. For the case of Doppler broadening $\Delta\nu_D$ is given by[47]

$$\Delta\nu_D = (8\ln(2)RT/M\lambda^2)^{1/2} \quad (34),$$

where R is the universal gas constant, T is the temperature in degrees Kelvin, M is the molecular weight and λ is the wavelength of the absorption transition. In the case of Lorentz broadening $\Delta\nu_L$ is given by[48]

$$\Delta\nu_L = (2)^{1/2} v N d^2 \quad (35),$$

where v is the velocity of the buffer gas atoms, N is the number density of the buffer gas atoms and d is an estimate of the atomic diameter ($d \simeq 3 \times 10^{-8}$ cm).[49] In the case of Holtsmark broadening $\Delta\nu_H$ is given by an expression similar to that for Lorentz broadening. That is,

$$\Delta\nu_H = (2)^{1/2} v N d^2 \quad (36),$$

where v is now the velocity of the absorbing atoms, N is the number density of the absorbing atoms and d is again an estimate of the atomic diameter ($d \simeq 3 \times 10^{-8}$ cm). The following Tables list the values of $\Delta\nu$ for the various line broadening phenomena.

TABLE 4

NATURAL BROADENING ABSORPTION LINEWIDTH

Element	Wavelength (Å)	Linewidth (Hz)
Ca	4457	3.89×10^5
Ca	6162	5.49×10^6
Mg	5184	9.15×10^6

TABLE 5

DOPPLER BROADENING ABSORPTION LINEWIDTH

Element	Wavelength (Å)	Temperature (°K)	Linewidth (Hz)
Ca	4457	850	2.21×10^9
Ca	6162	850	1.60×10^9
Mg	5184	800	2.37×10^9

TABLE 6

COLLISION BROADENING ABSORPTION LINEWIDTH

Element	Buffer Gas[+]	Temperature (°K)	Linewidth (Hz)
Ca	He	850	6.64×10^8
Ca	Ne	850	2.95×10^8
Ca	Ar	850	2.10×10^8
Mg	He	800	6.84×10^8
Mg	Ne	800	3.04×10^8
Mg	Ar	800	2.16×10^8

[+]The buffer gas pressure was equal to 100 Torr.

TABLE 7

HOLTSMARK BROADENING ABSORPTION LINEWIDTH

Element	Vapor Pressure (Torr)	Temperature ($^{\circ}$K)	Linewidth (Hz)
Ca	0.01	850	1.02×10^{4}
Mg	0.1	800	1.42×10^{5}

An examination of these tables indicates that the principal sources of broadening of the absorption line are Doppler and Lorentz broadening. The functional form of $F(\nu)$ in the cases of Doppler and Lorentz broadening will therefore now be discussed.

a. Doppler Broadening.

The phenomenon of Doppler broadening of an absorption or emission line is due to the motion of the nucleus of the atom. The functional form of the Doppler broadened lineshape function, $F_D(\nu)$, is given by[50]

$$F_D(\nu) = C \exp\left(-\left(2(\nu - \nu_{21})(\ln(2))^{1/2}\right)/\Delta\nu_D^2\right) \quad (37),$$

where C is some constant, ν_{21} is the resonant frequency of the absorption or emission line and $\Delta\nu_D$ is the Doppler linewidth. The constant, C, may be determined by the normalization condition

$$\int_{-\infty}^{\infty} F_D(\nu)\, d\nu = 1 \quad (38).$$

However, if the substitution

$$\omega = \left[2(\nu - \nu_{21})(\ln(2))^{1/2}\right]/\Delta\nu_D \quad (39)$$

is made the normalized expression for $F_D(\omega)$ is given by

$$F_D(\omega) = \left\{2(\ln(2)/\pi)^{1/2} \exp(-\omega^2)\right\}/\Delta\nu_D \qquad (40).$$

Substitution of this expression into the equation for the absorption coefficient, k_ν, yields

$$k_\nu = \left\{2k_0(\ln(2)/\pi)^{1/2} \exp(-\omega^2)\right\}/\Delta\nu_D \qquad (41).$$

b. Collisional or Lorentz Broadening

Collisions between excited atoms and foreign gas molecules can be an important cause of the broadening of emission or absorption lines. A thorough treatment of this effect is given in the article by Weisskoff and Wigner.[51] The functional form of the collision broadened lineshape function, $F_C(\nu)$, is given by[52]

$$F_C(\nu) = Q/\left\{(2(\nu-\nu_{21})/\Delta\nu_L)^2 + 1\right\} \qquad (42),$$

where ν is the frequency, ν_{21} is the resonant frequency of the transition, Q is a constant and $\Delta\nu_L$ is the number of broadening collisions per second per absorbing atom. The constant, Q, may be determined from the normalization condition given by equation (38).

After normalization $F_C(\nu)$ becomes

$$F_C(\nu) = (2/\pi\Delta\nu_L)/\left\{(2(\nu-\nu_{21})/\Delta\nu_L)^2 + 1\right\} \qquad (43).$$

For the case of pure collisional broadening k_ν becomes

$$k_\nu = (2k_0/\pi\Delta\nu_L)/\{(2(\nu-\nu_{21})/\Delta\nu_L)^2+1\} \qquad (44).$$

We have yet to consider the case when both Doppler and collisional broadening occur. This situation gives rise to a composite lineshape called the Voigt profile which will be the next topic for discussion.

c. Effect of Combined Doppler and Lorentz Broadening

Thus far the sources of broadening of absorption or emission lines have been independently considered. However, under actual experimental conditions both Doppler and collisional broadening may be present. The functional form of $F(\nu)$ due to the presence of both types of broadening mechanisms may be determined as follows. The Doppler and collisional broadening processes are considered to independently broaden the absorption line. Each infinitesimal frequency interval of the collision broadened curve is considered to be broadened by Doppler broadening. Consider a frequency band a distance, $\nu - \nu_{21}$, from the center of a line exhibiting collision broadening. A variable distance, δ, from the point $\nu - \nu_{21}$ is chosen to represent Doppler broadening of this frequency band. The combined probability of a transition occurring at a frequency $\nu + d\nu$ about a central frequency ν is given by[53]

$$F_T(\nu) = \frac{a}{\pi}\int_{-\infty}^{\infty}\frac{\exp(-y^2)\,dy}{(a^2+(\omega-y)^2)} \qquad (45),$$

where

$$\omega = \left\{2(\nu - \nu_{21})\,(\ell n(2))^{1/2}\right\}/\Delta\nu_D \qquad (39),$$

$$y = \left\{2\delta\,(\ell n(2))^{1/2}\right\}/\Delta\nu_D \qquad (46)$$

and

$$a = \left\{(\ell n(2))^{1/2}\Delta\nu_L\right\}/\Delta\nu_D \qquad (47).$$

This expression for the absorption lineshape function, $F_T(\nu)$, is sometimes called the Voigt profile. In this case k_ν is given by

$$k_\nu = \frac{k_0 a}{\pi}\int_{-\infty}^{\infty}\frac{\exp(-y^2)\,dy}{(a^2+(\omega-y)^2)} \qquad (48).$$

The final quantity to be investigated before evaluating the expression for the absorption, A, is the emission lineshape, I_ν. This investigation will occur in the next section.

4. The Emission Profile

The frequency distribution of the light intensity emitted by a radio frequency discharge lamp may take one of several functional forms. The emission lines may be broadened by Doppler, natural, collisional and Holtsmark broadening. A comparison of the linewidths caused by these broadening phenomena would help to determine the principal

cause of broadening of the emission line. These values are listed in Tables 8 through 11.

TABLE 8

NATURAL LINEWIDTH OF THE EMISSION LINE

Element	Wavelength (Å)	Linewidth (Hz)
Ca	4457	3.89×10^5
Ca	6162	5.49×10^6
Mg	5184	9.15×10^6

TABLE 9

DOPPLER LINEWIDTH OF THE EMISSION LINE

Element	Wavelength (Å)	Temperature (°K)	Linewidth (Hz)
Ca	4457	693	2.00×10^9
Ca	6162	693	1.45×10^9
Mg	5184	580	2.02×10^9

TABLE 10

COLLISIONAL LINEWIDTH OF THE EMISSION LINE

Element	Buffer Gas+	Temperature (°K)	Linewidth (Hz)
Ca	Ar	693	5.82×10^6
Mg	Ar	580	6.36×10^6

+Buffer gas pressure ≈ 5 Torr.

TABLE 11

HOLTSMARK LINEWIDTH OF THE EMISSION LINE

Element	Vapor Pressure (Torr)	Temperature (^{o}K)	Linewidth (Hz)
Ca	10^{-5}	693	12
Mg	10^{-5}	580	17

The predominant effect is seen to be Doppler Broadening. Therefore, an emission lineshape of the following form may be assumed[54]

$$I_\nu = I_0 \exp(-\omega^2/\alpha^2) \qquad (49),$$

where I_0 is the average incident intensity,

$$\omega = \{2(\nu - \nu_{21})(\ln(2))^{1/2}\}/\Delta\nu_D \qquad (39)$$

and

$$\alpha = \frac{\text{Emission line breadth}}{\text{Absorption line breadth}} \qquad (50)$$

($\alpha \simeq 0.85$ in this investigation).

The functional form of I_ν given by equation (49) will be used in the evaluation of the absorption, A, given by equation (6).

5. The Time Dependent Absorption Signal

The absorption, A, is given by the equation

$$A = 1 - \frac{\int_{-\infty}^{\infty} I_\nu \exp(-k_\nu \ell)\, d\nu}{\int_{-\infty}^{\infty} I_\nu\, d\nu} \qquad (6).$$

This expression will now be evaluated for the case in which the principal source of broadening of the absorption lineshape is Doppler broadening. The absorption, A, will also be evaluated for the case of combined Doppler and Lorentz broadening of the absorption line. In each case the expression for the absorption will be seen to depend on the observed lifetime of the $^3P_1$ level, Γ.

Case 1: Doppler emission and absorption profiles.

In this case the assumption is made that both the emission lineshape of the R.F. discharge lamp, I_ν, and the absorption coefficient of the atomic gas in the absorption cell are broadened by the Doppler effect. That is, I_ν is given by

$$I_\nu = I_0 \exp(-\omega^2/\alpha^2) \tag{49}$$

and k_ν is given by

$$k_\nu = \left\{2 k_0 (\ln(2)/\pi)^{1/2} \exp(-\omega^2)\right\}/\Delta\nu_D \tag{41}.$$

In this case equation (6) becomes

$$A = 1 - \frac{\int_{-\infty}^{\infty} I_0 \exp(-\omega^2/\alpha^2) \exp(-\sigma \ell \exp(-\omega^2))\, d\omega}{\int_{-\infty}^{\infty} I_0 \exp(-\omega^2/\alpha^2)\, d\omega} \tag{51},$$

where

$$\sigma = \left\{2 k_0 (\ln(2)/\pi)^{1/2}\right\}/\Delta\nu_D$$

This expression for A is evaluated in terms of a power

series[55]

$$A = 1 - \sum_{m=0}^{\infty} \frac{(-1)^m (\sigma \ell)^m}{m!\,(\alpha^2 m + 1)^{1/2}} \tag{52}$$

or

$$A = 1 - \sum_{m=0}^{\infty} \frac{(-1)^m (C n_j(0) \exp(-t/\Gamma))^m}{m!\,(\alpha^2 m + 1)^{1/2}} \tag{53},$$

where

$$C = \ell B_{12} h \nu_{21} / (c \eta V) \tag{54}$$

and $n_j(0)$ is the population at time, t = 0, of the ^3P_j (j = 0,1 and 2) level. Equation (53) explicitly shows that the absorption is time dependent. In the limit that $\alpha \to 0$ (i.e., the emission linewidth is much smaller than the absorption linewidth) A is given by

$$A = 1 - \exp(-C n_j(0) \exp(-t/\Gamma)) \tag{55}.$$

If one further assumes that $C n_j(0) < 1$ ($C n_j(0) \approx .2$ in this work) then equation (55) may be written as

$$A \approx 1 - C n_j(0) \exp(-t/\Gamma) \tag{56}.$$

Thus we have three time dependent models for the absorption signal given by equations (53), (55) and (56).

Case 2: Doppler broadened emission profile with a Voigt absorption profile

In this case the emission line profile of the R.F. discharge lamp is assumed to be Doppler broadened while the the absorption coefficient of the atomic gas has a lineshape given by the Voigt profile. That is, I_ν is again given by

$$I_\nu = I_0 \exp(-\omega^2/\alpha^2) \tag{49},$$

while k_ν is written as

$$k_\nu = \frac{k_0 a}{\pi} \int_{-\infty}^{\infty} \frac{\exp(-y^2)\,dy}{(a^2 + (\omega - y)^2)} \tag{48}.$$

Under these conditions the expression for A becomes

$$A = 1 - \frac{\int_{-\infty}^{\infty} (I_0 \exp(-\omega^2/\alpha^2) \exp(-C' n_j(0) k_\nu \exp(-t/T)))\,d\omega}{\int_{-\infty}^{\infty} I_0 \exp(-\omega^2/\alpha^2)\,d\omega} \tag{57}$$

in which

$$C' = (a \ell B_{12} h \nu_{12})/(\pi c \eta V) \tag{58}.$$

The above expression for A must be integrated numerically from tabulated values[56] of equation (48). Thus, equation (57) is also seen to depend on the population of the ^3P_j (j = 0, 1 and 2) level as a function of time.

It has been shown that there are four expressions for the time dependent absorption, A. If Doppler and collisional broadening of the absorption lineshape are both

important effects then the integral expression for A specified by equation (57) must be used. If only Doppler broadening of the absorption profile is important the expression for A is given by the sum indicated in equation (53). If the further assumption that the emission linewidth is much less than the absorption linewidth is made then the expression for A given by equation (55) may be used. Finally, in the limit that $Cn_j(0) < 1$ (i.e., weak absorption) the single exponential expression given by equation (56) may be employed. The time dependence of the absorption was simulated with the aid of a computer. All four models of the absorption discussed above were investigated. Graphs of equations (57), (53), (55) and (56) plotted as a function of time are shown in Figures 4 and 5. In Figure 4 the absorption, A, is equal to 20% of the incident intensity while in Figure 5, A equals 12% of the incident intensity. The observed lifetime, Γ, was chosen to be 0.39 msec in each case and the functions all had the same initial amplitude at t = 0. One can see from Figures 4 and 5 that for 12-20% absorption the various expressions for A yield curves that almost coincide. In this investigation the bulk of the absorption signals analyzed were estimated to have been for less than 20% absorption. Figure 6 shows a plot of the integral expression for A superimposed upon the single exponential expression. The lifetime of the single exponential function was varied until the curves coincided as closely as possible. The lifetime used in the

FIGURE 4

Computer simulation of 4 theoretical absorption models plotted versus time. In curve (a) the absorption, A, is given by the equation

$$A = C n_j(0) \exp(-t/\Gamma) .$$

In curve (b) the absorption is of the functional form

$$A = 1 - \sum_{m=0}^{10} \frac{(-1)^m (C n_j(0) \exp(-t/\Gamma)}{m! (\alpha^2 m + 1)^{1/2}} .$$

The absorption is given by the expression

$$A = 1 - \frac{\int_{-\infty}^{\infty} I_0 \exp(-\omega^2/\alpha^2) \exp(-C' n_j(0) h_\nu \exp(-t/\Gamma)) d\omega}{\int_{-\infty}^{\infty} I_0 \exp(-\omega^2/\alpha^2) d\omega}$$

in curve (c). A plot of the theoretical absorption model

$$A = 1 - \exp(-C n_j(0) \exp(-t/\Gamma))$$

is depicted in curve (d). In each instance the absorption is 20% of the incident intensity.

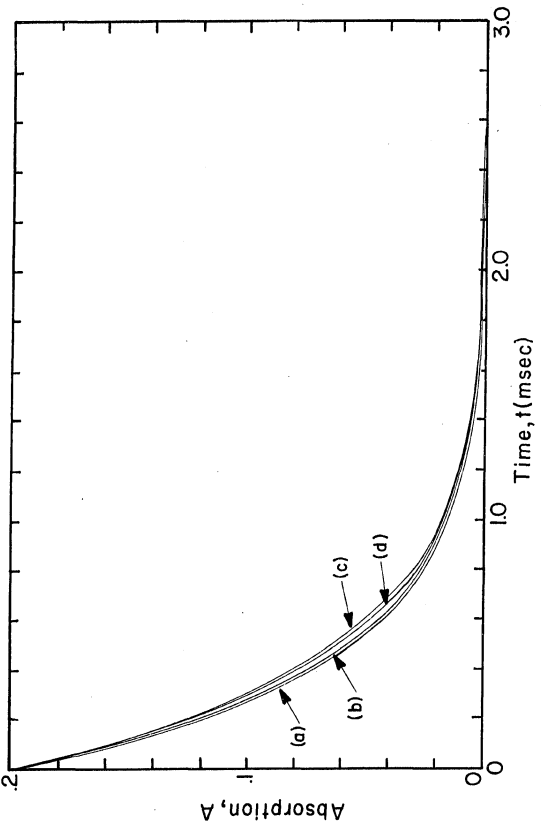

FIGURE 5

Computer simulation of 4 theoretical absorption models plotted versus time. The curves for the models $A = Cn_j(0)\exp(-t/\Gamma)$ and

$$A = 1 - \sum_{m=0}^{40} \frac{(-1)^m (Cn_j(0)\exp(-t/\Gamma))^m}{m!\,(m\alpha^2 + 1)^{1/2}}$$

coincide and correspond to curve (a). Curve (b) is a graph of the absorption when its functional dependence is given by

$$A = 1 - \frac{\int_{-\infty}^{\infty} I_0 \exp(-\omega^2/\alpha^2)\exp(-C'n_j(0)h_{\nu}\exp(-t/\Gamma))\,d\omega}{\int_{-\infty}^{\infty} I_0 \exp(-\omega^2/\alpha^2)\,d\omega}$$

Curve (c) is a graph of the absorption which is given by the expression

$$A = 1 - \exp(-Cn_j(0)\exp(-t/\Gamma)) .$$

In each instance the absorption is 12% of the incident intensity.

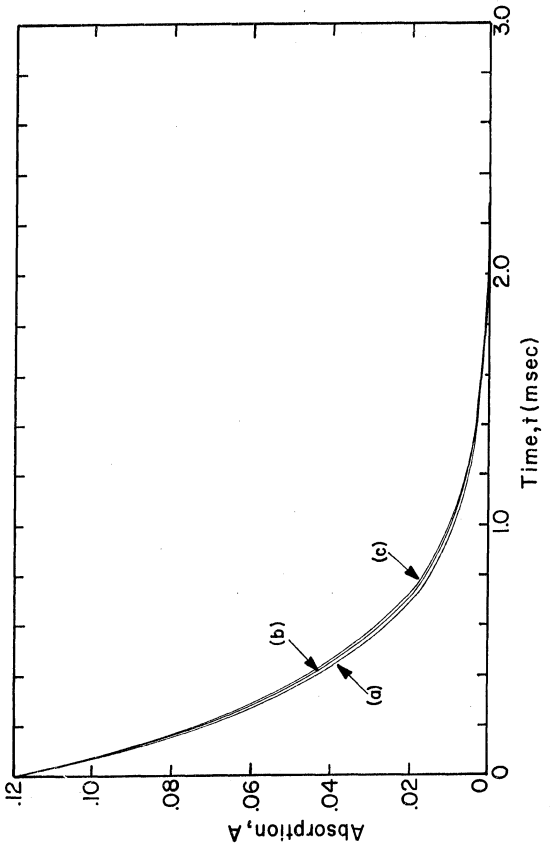

FIGURE 6

Graph of the integral and exponential absorption models. Curve (a) is a graph of the equation

$$A = 1 - \frac{\int_{-\infty}^{\infty} I_0 \exp(-\omega^2/\alpha^2)\exp(-k_\nu C' n_j(0) \exp(-t/\Gamma))\, d\omega}{\int_{-\infty}^{\infty} I_0 \exp(-\omega^2/\alpha^2)\, d\omega} .$$

Curve (b) is a graph of the equation $A = C n_j(0) \exp(-t/\Gamma)$. The lifetime, Γ, used in the equation for curve (a) was 0.39 msec. The lifetime of the expression used to plot curve (b) was varied to achieve coincidence of the two curves. The best fit was given by $\Gamma = 0.4025$ msec.

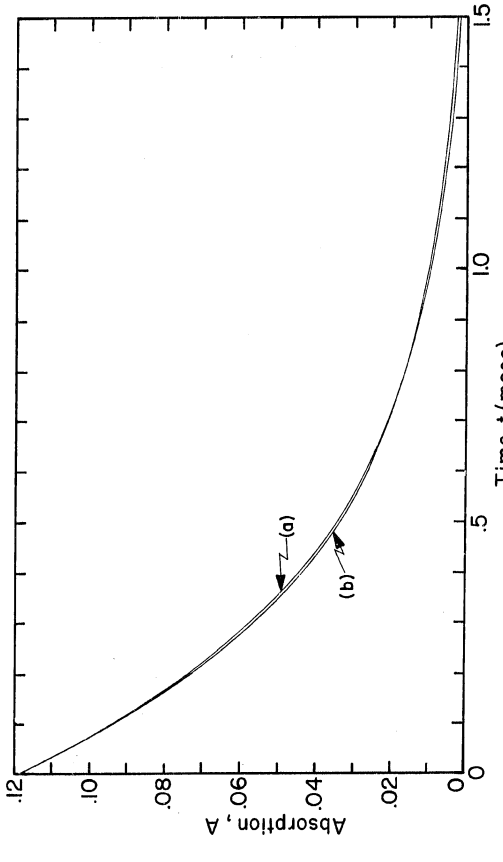

FIGURE 7

Photograph showing computer fit to experimental data. The upper trace shows the data and the fit to the function

$$A = 1 - \sum_{m=0}^{4} \frac{(-1)^m (\mathcal{C} n_j(0) \exp(-t/I'))^m}{m!\,(m+1)^{1/2}}$$

The middle trace is a fit to the expression

$$A = 1 - \exp(-\mathcal{C} n_j(0) \exp(-t/I')) \ .$$

The lower trace is a fit to the expression

$$A = \mathcal{C} n_j(0) \exp(-t/I') \ .$$

integral expression was 0.39 msec while the lifetime of the single exponential function was found to be 0.4025 msec in order for coincidence to be achieved. This difference in the lifetime values is on the order of 3%.

Some of the Ca experimental data were fit by the computer using equations (53), (55) and (56) as the theoretical models for the absorption, A. Figure 7 is a photograph of the same experimental data fit to these models for the absorption. The data was analyzed by a PDP-LAB8/E computer and the data (small dots) and the final fits (solid curves) were displayed on an oscilloscope. The upper trace shows the data and final fit for the summation expression given by equation (53). In this case α was taken to be 1.0 and only four terms were taken in the sum. It was found that the series converges rapidly and that the first four terms gave a sufficiently accurate estimate for A. This fit yielded a value of 0.4056 msec for τ, the natural lifetime. The middle trace was a fit to the expression for A given by equation (55). This fit yielded a value for the lifetime, τ, of 0.4055 msec. The lowest trace yields a value of τ equal to 0.4063 msec. In this case the data was fit to equation (56), the simple exponential function. These values agree to within 0.1%. Therefore, since only a slight error would be made by using equations (55) and (56) instead of the more exact integral or sum expressions for A, the bulk of the experimental data was analyzed using these expressions. Thus, the final expressions used to fit the

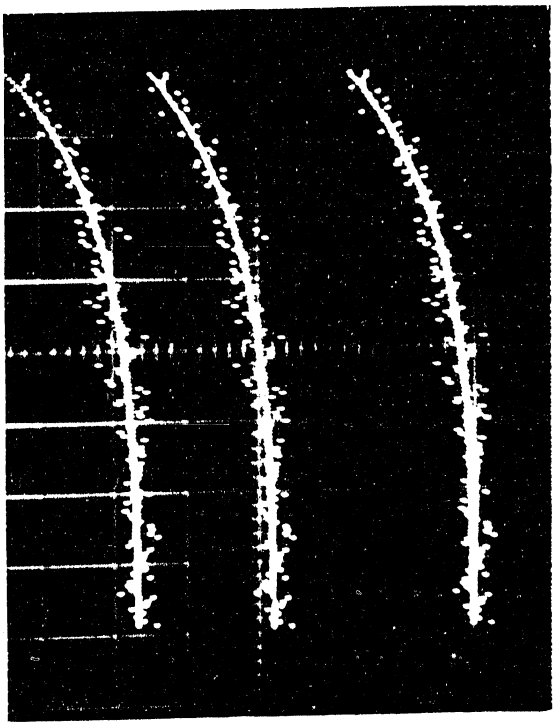

experimental absorption signals were

$$A = 1 - \exp(-C n_j(0) \exp(-t/\Gamma)) \qquad (55)$$

and

$$A = C n_j(0) \exp(-t/\Gamma) \qquad (56).$$

It should be noted that both of these expressions are dependent on the population of the ^3P_j (j = 0,1 and 2) level as a function of time and that A must be multiplied by the intensity of the incident radiation in order to yield the magnitude of the absorption signal.

CHAPTER III

EXPERIMENTAL MATERIALS AND METHODS

The experimental procedures and apparatus employed in this investigation will be discussed in this chapter. The first section of this chapter will describe the experimental arrangement and procedures used to create, sample and analyze absorption signals produced by the absorption of radiation by atoms in the Ca and Mg ^3P levels. These absorption measurements provided the greater part of the experimental data used to determine the natural lifetime of the Ca and Mg $^3P_1$ metastable level. The discussion of the absorption experiments will also include a description of the two theoretical models for the absorption signals used in this investigation as well as the least squares fitting routines used by the PDP-LAB8/E computer to determine the natural lifetime, τ.

The validity of the absorption measurement technique is dependent on the assumption that the populations of the Ca and Mg ^3P levels corresponded to those expected under conditions of thermal equilibrium. The measurements undertaken to verify this assumption will be described in the second section of this chapter.

The lifetime of the Mg $^3P_1$ level was also deter-

mined by measurements of the fluorescence from the excited $^3P_1$ atoms. These measurements were undertaken to corroborate the results obtained in the absorption measurements. The experimental procedures employed in making these fluorescence measurements as well as the data reduction by the computer will be described in the third section of this chapter.

A detailed description of the experimental apparatus will be found in the fourth section of this chapter. This will be followed by a discussion of the sample preparation procedure and the vacuum-gas handling system in the last section of this chapter.

A. Absorption Signal Measurements

The purpose of these measurements was to determine the lifetime of the $^3P_1$ level of Ca and Mg. The relevant energy level diagrams for these elements are shown in Figures 8 and 9. The lifetime of the $^3P_1$ level was determined by measuring the absorption of light from a radio frequency discharge lamp by atoms in the $^3P_2$, $^3P_1$ or $^3P_0$ levels as a function of time. The absorption decreased with time as the atoms in the $^3P_1$ level returned to the ground state.

The measurement process was similar in both the Ca and Mg experiments. In both of these experiments the amount of absorption out of either the $^3P_2$ or the $^3P_1$ or the $^3P_0$ level was monitored as a function of time. In the

FIGURE 8

Relevant energy-level structure of Ca. The 6573-Å line corresponds to the light emitted by the laser. The lines from the $^3P_2$, $^3P_1$, and $^3P_0$ levels to higher energy levels correspond to the wavelengths emitted by the radio frequency discharge lamp and absorbed by excited Ca atoms in the absorption cell.

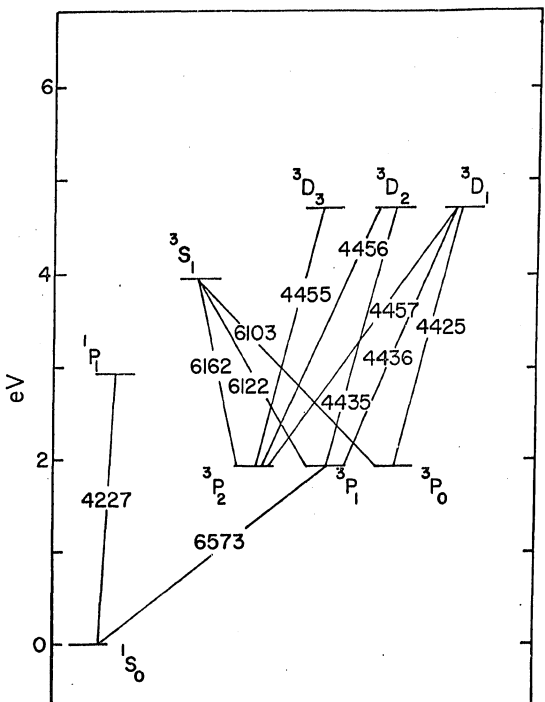

FIGURE 9

Relevant energy-level structure of Mg. The 4571-Å line corresponds to the light emitted by the laser. The lines from the $^3P_2$, $^3P_1$, and $^3P_0$ levels to the higher energy levels correspond to the wavelengths emitted by the radio frequency discharge lamp and absorbed by excited Mg atoms in the absorption cell.

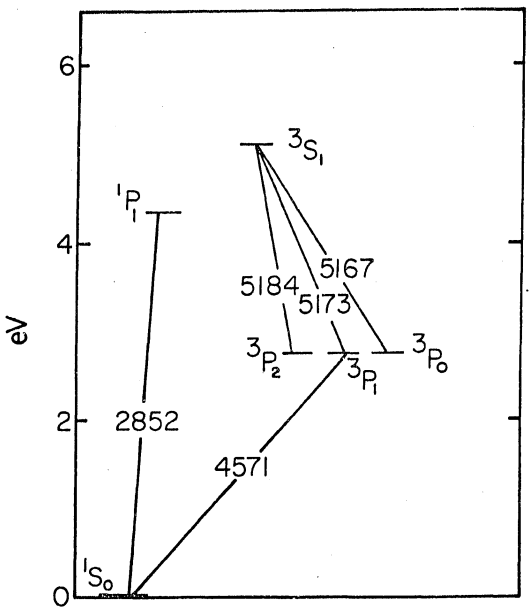

Mg measurements this involves monitoring the absorption at the wavelengths corresponding to the transitions $^3P_2 \leftrightarrow {}^3S_1$, $^3P_1 \leftrightarrow {}^3S_1$ and $^3P_0 \leftrightarrow {}^3S_1$ (See Figure 9). In the Ca measurements the absorption out of the $^3P_2$ level was monitored at the wavelengths corresponding to the transitions $^3P_2 \leftrightarrow {}^3D_3$, $^3P_2 \leftrightarrow {}^3D_2$ and $^3P_2 \leftrightarrow {}^3D_1$ (The wavelengths of these transitions only differ by an angstrom from each other and could not be resolved with the spectrophotometer used in this investigation). The absorption out of the $^3P_1$ level in Ca was monitored at the wavelengths corresponding to the $^3P_1 \leftrightarrow {}^3D_2$ and $^3P_1 \leftrightarrow {}^3D_1$ transitions (Once again the spectrophotometer was unable to resolve the two lines). Finally, the absorption out of the Ca $^3P_0$ level was measured at the wavelength corresponding to the transition $^3P_0 \leftrightarrow {}^3D_1$. (See Figure 8).

The experimental arrangement is shown in Figure 10. A 1 μsec pulse of radiation corresponding to the transition $^1S_0 \leftrightarrow {}^3P_1$ in either Ca or Mg was produced by the dye laser. The radiation passed through a beam expander which increased the diameter of the laser beam by a factor of five. The laser beam then passed through mirror M-1 and was incident of the Tantalum lined quartz absorption cell containing either Ca or Mg. The sample was attached to a vacuum-gas handling system through which an inert buffer gas was introduced into the absorption tube. The buffer gas prevented rapid diffusion of Ca or Mg vapor to the walls and kept the cell windows clean. The gas pressure was varied from

FIGURE 10

Block diagram of experimental arrangement for absorption measurements.

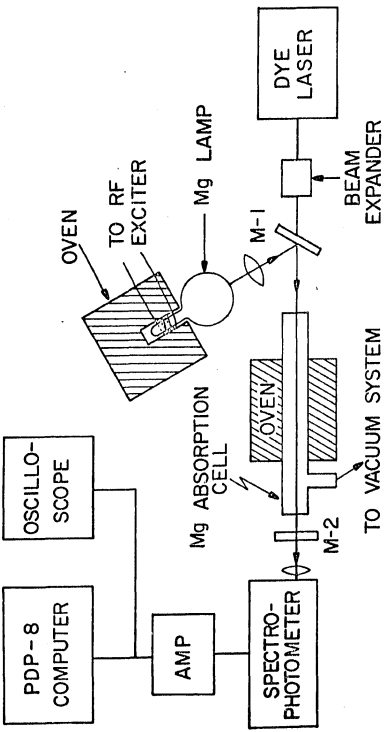

10 to 600 Torr by means of the vacuum-gas handling system. This system also included a capacitive manometer which enabled measurements of the gas pressure to be made. The absorption cell was heated in an oven to temperatures ranging from 500 to 650 ^{o}C. Heating the cell produced Ca or Mg vapor with the majority of the atoms being in the ground state. The laser radiation excited some of the atoms from the $^{1}S_{0}$ ground state to the $^{3}P_{1}$ excited level. Light from a radio frequency discharge lamp corresponding to the spectrum of the element being investigated was reflected from mirror M-1 and passed collinearly with the laser beam through the absorption cell. Mirror M-2 at the output end of the absorption cell reflected 95% of the laser radiation back through the cell for a second transit, while transmitting the light from the discharge lamp. The lamp light was focused on the entrance slit of a 1/2-m spectrophotometer by a converging lens. A glass filter in front of the slit attenuated any remaining laser light but allowed the discharge lamp light to pass. The spectrophotometer was adjusted to transmit the lamp light to its exit slit. The absorption out of the $^{3}P_{2}$, $^{3}P_{1}$ and $^{3}P_{0}$ levels was selectively observed by adjusting the spectrophotometer to the proper wavelength. A photomultiplier tube measured the amount of light emerging from the exit slit. A current pulse was produced by the photomultiplier which in turn created a potential difference across a resistor. The potential difference created by the current pulse was amplified by a D.C.

amplifier. An oscilloscope and the input to the Analog-to-Digital Converter of a PDP-LAB8/E computer were connected in parallel with the amplifier output. The absorption signal was displayed on the oscilloscope while the voltage was simultaneously measured by the Analog-to-Digital Converter. The voltage and the time of sampling were stored in the memory of the PDP-LAB8/E computer for further processing.

In Chapter II two different equations for the absorption were derived. Each of these equations was shown to be a function of the lifetime of the $^3P_1$ level. The data analysis procedure will be explained for each of these two models for the absorption signal.

For most of the Ca data the absorption signal was taken to be of the form

$$V(t) = A'(1 - \exp(-Cn_j(0)\exp(-t/\Gamma)))+B \qquad (59).$$

In the above equation V(t) is the measured voltage, t is the time, Γ is the observed lifetime, and B is the D.C. baseline of the light. The constant, C, was defined in Chapter II and is given by

$$C = (l B_{12} h\nu_{21})/(c\eta V) \qquad (54).$$

The quantity $n_j(0)$ is the population of the ^3P_j (j=0,1,2) level at t = 0 and A' is given by

$$A' = (V(0) - B)/(1 - \exp(-Cn_j(0))) \qquad (60),$$

in which V(0) is the voltage at time, t = 0. The computer

was programmed to sample the voltage of the absorption signal, as a function of time, calculate and subtract the baseline from the measured voltage and store the corrected voltages and times in an array. A least squares fit of the data to the function

$$V(t) - B = A'\left\{1 - \exp(-C n_j(0) \exp(-t/\Gamma))\right\} \qquad (61)$$

was performed to find C and Γ. The fit was accomplished by varying C and Γ independently until the sum of the squares of the differences in the absorption predicted by the model and given by the data was less than a preset minimum. The observed lifetime, Γ, was then multiplied by β to obtain the natural lifetime, τ.

For the remainder of the Ca and all of the Mg experiments the absorption signal was taken to have the functional form

$$V(t) = A'' \exp(-t/\Gamma) + B \qquad (62),$$

where V(t) is the measured voltage, A" is the amplitude coefficient, B is the D.C. baseline of the light, t is the time, and Γ is the observed lifetime. A signal averaging program was also employed when equation (62) was taken as the absorption model. The computer was programmed to measure an absorption signal, calculate and subtract the baseline from the measured voltages measured and store the corrected voltages and times in an array. A new signal was acquired and its baseline was determined from the voltage

measurements. The baseline was then subtracted from all the new voltage data. The new signal voltages were added to those previously acquired and data collection proceeded in this manner until N signals had been obtained. The sums of the voltages at each instant of time were then divided by the total number of signals, N, and a least squares fit was performed on the signal averaged data to determine A" and Γ. This was accomplished by varying A" and Γ independently until the sum of the squares of the differences between the values predicted by the model and the data was less than a preset minimum. The observed lifetime, Γ, was then multiplied by β to obtain the natural lifetime, τ. The results of these measurements will be presented in Chapter IV. A listing and discussion of the program used to perform the signal averaging and the least squares fit is presented in Appendix II. It should be noted that the same least squares fitting routine was used in fitting data to both absorption models.

B. Thermal Equilibrium Measurements

In section B.2 of Chapter II the equation for the time dependence of the ^3P system population was derived. A major assumption in this derivation was that the populations of the $^3P_2$, $^3P_1$ and $^3P_0$ levels were in thermal equilibrium. Measurements were made to verify this assumption experimentally. As in Chapter II, let the populations of the $^3P_2$, $^3P_1$ and $^3P_0$ levels be denoted by n_2, n_1 and n_0. Equations

(17), (18) and (19) suggest that the ratios of the populations of the ^3P fine structure levels should be equal to the ratios of the constants, α, β and γ (i.e., $n_2:n_1:n_0 = \gamma:\beta:\alpha$). If the populations were in thermal equilibrium at some temperature, T, the values of α, β and γ would be given by equations (26), (27) and (28). Therefore, in order to verify the assumption of thermal equilibrium in the sample, the populations of the $^3P_2$, $^3P_1$ and $^3P_0$ levels must be found. The ratios $n_2:n_1:n_0$ may then be formed and compared to the ratios $\gamma:\beta:\alpha$ as given by equations (28), (27) and (26). The amplitude of the absorption out of the $^3P_2$, or $^3P_1$ or $^3P_0$ level is directly proportional to the population of the level if the single exponential absorption formula, equation (62), is assumed to be true. As mentioned in Chapter II, the absorption, A, must be multiplied by the incident light intensity in order to yield the magnitude of the absorption signal. Therefore, if the amplitudes of the absorption signals out of the $^3P_2$, $^3P_1$ and $^3P_0$ levels are measured and divided by the respective values of the incident intensity of the radiation absorbed, the ratios of these normalized amplitudes will give the ratios of the populations of the ^3P levels $n_2:n_1:n_0$.

The experiment to verify the condition of thermal equilibrium was conducted in the following manner. First, the incident light intensity was measured. Light from a Ca or Mg discharge lamp was reflected by mirror M-1 into the Ca or Mg absorption cell. The light passed through the

cell, through mirror M-2 and entered the spectrophotometer. The spectrophotometer was adjusted to measure the intensity of the lamp light corresponding to the transitions $^3P_2 \leftrightarrow {}^3D$, $^3P_1 \leftrightarrow {}^3D$ and $^3P_0 \leftrightarrow {}^3D$ in the case of Ca and $^3P_2 \leftrightarrow {}^3S_1$, $^3P_1 \leftrightarrow {}^3S_1$ and $^3P_0 \leftrightarrow {}^3S_1$ in the case of Mg. The intensity of each of these lines was measured. The next part of the experiment involved measuring the amplitude of the absorption out of the Ca or Mg $^3P_2$, $^3P_1$ or $^3P_0$ levels after these levels were populated by the dye laser. The Mg measurements were made by taking photographs of the trace of the absorption signals displayed on the oscilloscope. The Ca measurements were performed in exactly the same manner as described in section A of this chapter. In this case, however, the computer was programmed to determine the average initial amplitudes of the absorption signals. The Ca lamp light employed was that corresponding to the transitions from the ^3P levels to the $^3S_1$ level (See Figures 8 and 9). An average amplitude was calculated by the computer for the absorption signal corresponding to each of the above transitions. These average amplitudes were then normalized by dividing the amplitude of the absorption signal by the incident lamp intensity at the same wavelength. The ratios of the normalized amplitudes were then taken to obtain the ratio of the populations of the ^3P levels. The results of these measurements will be presented in Chapter IV.

FIGURE 11

Block diagram of the experimental arrangement for Fluorescence measurements.

C. Fluorescence Lifetime Measurements

Measurements of the lifetime of the Mg $^3P_1$ level were also made by monitoring the fluorescence from the $^3P_1$ level as a function of time. We were unable to detect fluorescence from the Ca $^3P_1$ level. These fluorescence measurements were performed to corroborate the lifetime determinations made by the absorption techniques described in the first section of this chapter. The fluorescence from the $^3P_1$ excited level should vary with time as $\sim \exp(-t/\tau)$. In this expression τ is the natural lifetime of the $^3P_1$ level. However, as discussed in Chapters I and II, thermal mixing collisions occur between the atoms of the $^3P_2$, $^3P_1$ and $^3P_0$ fine structure levels. The transitions $^3P_2 \leftrightarrow {}^1S_0$ and $^3P_0 \leftrightarrow {}^1S_0$ are forbidden, making the $^3P_1 \leftrightarrow {}^1S_0$ transition the only mode of decay available to the atoms in the ^3P system. These effects result in an apparent lengthening of the observed lifetime. Thus, the time dependence of the fluorescence from the $^3P_1$ level is given by $\exp(-t/\Gamma)$. In this expression Γ is the observed lifetime. The relationship between the natural lifetime, τ, and the observed lifetime, Γ, is given by

$$\tau = \beta \Gamma \tag{32}$$

in which $\beta = 0.34$ for Mg.

A schematic diagram of the experimental arrangement is shown in Figure 11. In order to prevent laser

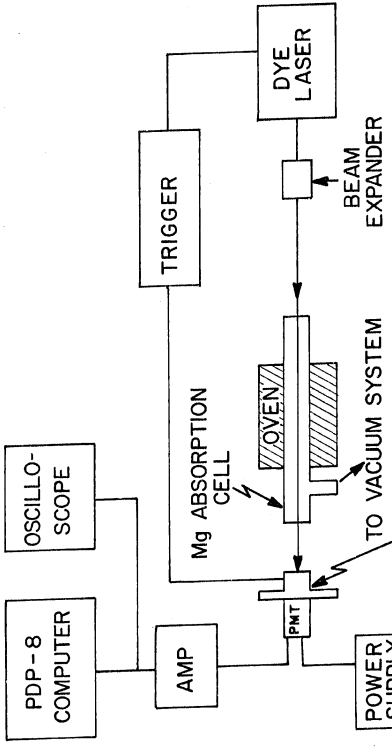

radiation from entering the photomultiplier tube, PMT, a triggering device was used to fire the laser and after a suitable time delay open a camera shutter positioned in front of the photomultiplier tube. When measurements were to be made a switch was closed which applied a 6 volt positive going pulse to the external triggering circuit of the dye laser. The dye laser then fired a 1 μsec pulse of coherent radiation corresponding to the transition $^3P_1 \leftrightarrow {}^1S_0$ in Mg. The laser light was expanded to five times its original diameter by a beam expander. The laser light excited atoms in the absorption cell from their ground state to the $^3P_1$ excited level. The atoms in the Mg $^3P_1$ excited level decay back to the ground state giving off light. The camera shutter protecting the photomultiplier tube was opened 10 to 20 msec after the laser had fired. The fluorescence from the Mg $^3P_1$ level was monitored as a function of time by the photomultiplier tube. The fluorescence signal was displayed on the oscilloscope and sampled by the Analog-to- Digital Converter of the mini-computer. The fluorescence signal had the functional form

$$V(t) = R \exp(-t/\Gamma) + B \qquad (63)$$

in which V(t) is the voltage, R is the amplitude coefficient of the signal, t is the time, Γ is the observed lifetime and B is the D.C. baseline of the light. The signal averaging and least squares fitting routines discussed in section A of this chapter were used to compute the natural lifetime, τ.

D. Apparatus

1. Dye Laser

A Phase-R model DL-32[57] flashlamp pumped dye laser was used in this experiment to excite atoms from their ground state to the $^3P_1$ metastable level. The laser had a quartz flashlamp which was coaxial to a tube through which dye was made to flow by means of a fluid pump. The optical cavity of the laser consisted of two mirrors and a diffraction grating. Coherent radiation was produced when a pulse discharge capacitor was charged to a high voltage, usually 18 kV, and was discharged through the coaxial flashlamp after being triggered by a spark gap. The light pulses produced by the laser can be made to vary in wavelength from 4000-Å to 6500-Å by a suitable choice of the dye solution. Once a dye was chosen the radiation from the laser could be tuned to within 0.5-Å of the desired wavelength by means of a diffraction grating. In this experiment two different lasing solutions were used. A 2×10^{-4} Molar solution of 7-Diethylamino-4-Methylcourmarin ($C_{14}H_{17}NO_2$)[58] with 200 proof Ethanol as the solvent was used to produce radiation at a wavelength of 4571-Å corresponding to the transition $^1S_0 \leftrightarrow {}^3P_1$ in Mg. A one-to-one mixture of a 5×10^{-5} Molar solution of Cresyl Violet Perchlorate ($C_{16}H_{12}ClN_3O_5$)[58] with a 4×10^{-5} Molar solution of Rhodamine 6G ($C_{28}H_{30}N_2O_3HCl$)[58] with 200 proof Ethanol as the common solvent was used to produce radiation at a wavelength of

6573-Å corresponding to the $^1S_0 \leftrightarrow {}^3P_1$ transition in Ca. The laser produces pulses of approximately 1 μsec duration and of about 0.1 Joules of energy and with a diameter of approximately 1 cm. The laser is capable of firing automatically once every second. The laser may also be fired manually or by an external triggering pulse.

2. Radio Frequency Discharge Lamp

The R.F. discharge lamp consisted of a round bottomed one-liter pyrex flask with the neck extended by a five inch piece of one-inch diameter pyrex tubing sealed at one end. A small stem of 8 mm pyrex tubing was affixed to the side of the flask. Calcium or Magnesium was placed into the neck of the lamp and the neck was inserted into a 4-inch long R.F. coil consisting of eight turns of 12 AWG enameled wire. The coil was housed in a firebrick[59] oven which was enclosed in an aluminum box. The lamp and oven arrangement is shown in Figure 12. The lamp was attached to a vacuum system by means of the 8 mm stem. After being evacuated, about 5 Torr of Research Grade Argon[60] was introduced into the lamp and a Heathkit Model DX-20 transmitter was connected to the R.F. coil in the oven. The Argon gas was then ionized with a Tesla coil and the discharge was maintained by the R.F. field in the coil. Thus, the coil and lamp provided the load for the transmitter. The lamp was heated in the oven by a horseshoe-shaped heating coil placed in the bottom of the oven. The lamp's temperature

FIGURE 12

Radio frequency discharge lamp and oven.

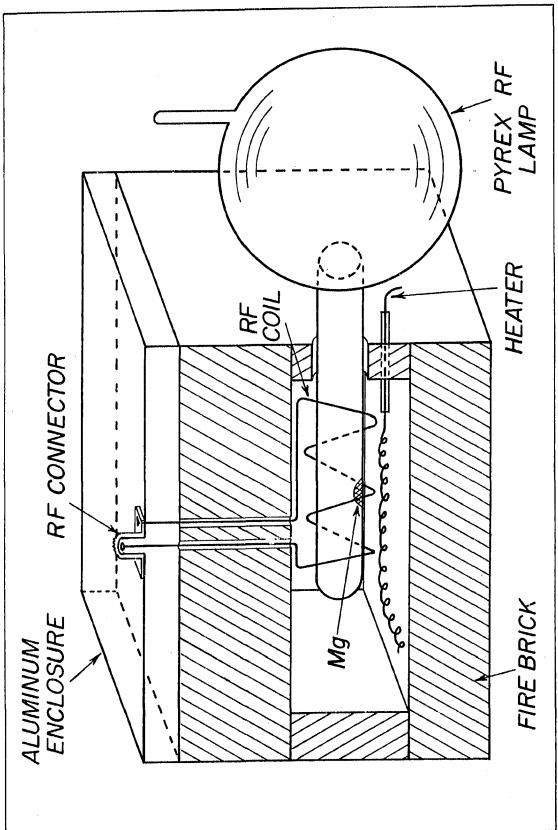

was monitored by a thermometer protruding into the oven through a hole in the aluminum enclosure. Heating the lamp produced Ca or Mg vapor. This atomic vapor underwent collisions with the ions present in the R.F. discharge thereby becoming excited to higher energy levels. The atoms decayed back to lower excited states and the ground state and emitted light. In actuality when the Ca or Mg is first heated only the characteristic lines of Na, from the glass are very intense. It was only after a reaction between the alkaline vapor and the glass had taken place impeding the liberation of the Na and the Mg or Ca had been outgassed by heating and ion bombardment that the spectrum of Ca or Mg became evident.It was not unusual to have had to cool the lamp, evacuate it and put in a fresh charge of Ar several times before sufficiently intense light was obtained. Once this condition had been fulfilled, however, a final charge of about 3 Torr of Ar was introduced into the lamp and it was sealed off. In actual operation a temperature was selected for the lamp which produced relatively stable operation. The degree of self-reversal of the lines emitted by the lamp was controlled by varying the lamp's operating temperature.

3. Optics

In the Ca experiment the mirror M-1[61] (See Figure 10) was specially coated to transmit 90% of the 6573-Å laser line while reflecting 95% of the lamp radiation bet-

ween 4000-Å and 6200-Å, enabling both beams to pass collinearly through the Ca absorption cell. Another mirror was placed between the absorption cell and the 1/2-m spectrophotometer. This mirror, M-2[61], was specially coated to transmit radiation between 4000-Å and 6200-Å while reflecting 95% of the 6573-Å laser line for a second transit of the absorption cell.

In the Mg experiment mirror M-1[61] was specially coated to transmit 90% of the 4571-Å laser line while reflecting 95% of the 5173-Å line again enabling both the lamp radiation and that of the laser to pass collinearly through the Mg absorption cell. Mirror M-2[61] was coated to transmit 90% of the 5173-Å line to the spectrophotometer while reflecting 95% of the 4571-Å laser line for a second transit of the absorption cell.

In the Mg experiment a commerical broadband yellow glass filter which absorbed strongly in the green region of the spectrum was used to absorb any residual laser light at 4571-Å which had not been reflected by Mg mirror M-2. This glass filter was employed to protect the spectrophotometer.

For the same reason a commerical broadband blue glass filter was used in the Ca experiment to absorb any residual laser light at 6573-Å, which had not been totally reflected by Ca mirror M-2, before it could reach the spectrophotometer.

A beam expander was used to expand the 1 cm diameter laser beam by a factor of five. This expansion pro-

duced a uniform intensity across the window of the absorption cell. In the preliminary work performed by Wright et al.[27] to determine the Mg $^3P_1$ lifetime a laser with a much smaller beam diameter was used. It was found that the narrow beam of this laser was capable of exciting a large number of atoms to the $^3P_1$ metastable level. These excited atoms were at first contained in a small volume. The excited atoms completely absorbed all of the light from the radio frequency discharge lamp in this volume. However, a number of excited atoms which had not absorbed radiation remained in the volume. As the remaining excited atoms diffused out of the excitation region, lamp light was once again available for absorption. This effect produced an absorption signal which actually grew for a short time before it began to decrease. This produced a distorted absorption signal. In order to prevent this effect, a beam expander was employed. The laser used in the present investigation had a much larger beam diameter. Hence the diffusion problem mentioned above was never a serious problem even when no beam expander was employed.

4. Sample Oven

The sample oven is shown in Figure 13. It consisted of a rectangular aluminum box without a top, 14.25 inches long, 8.25 inches wide and 9.5 inches high. This aluminum box was lined with firebricks to form an oven. The bricks at the front and back sides of the oven had a U-shaped slot

FIGURE 13

Sample Oven

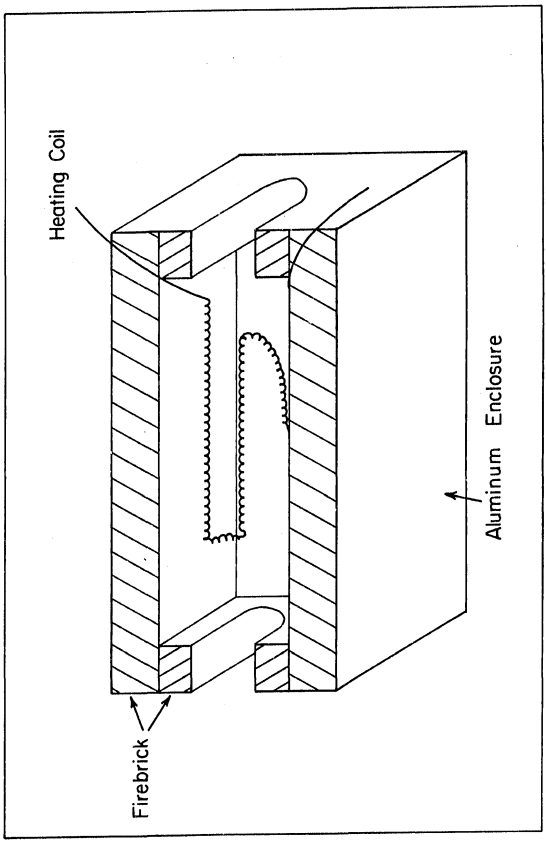

in them to form a cradle in which the sample rested. A wire heater was placed in the side and bottom bricks of the oven. This heater was connected to a 20 amp Variac. A firebrick with a hole in its center for a thermocouple rested on the side walls of the oven to form the top. Fiberfrax insulation[62] was used to fill in any heat leaks in the oven. A Platinum-Platinum 10% Rhodium thermocouple with its reference junction in ice water was used to measure the sample's temperature. The thermal emf produced in the thermocouple was measured by a John Fluke Model 801H Potentometric D,C. Voltmeter.

5. Signal Detection Apparatus

The absorption signals were detected by a 1/2-m spectrometer which had a RCA 4517 Photomultiplier tube monitoring the light emerging from the spectrometer's exit slit. The photomultiplier had a negative voltage of 1250 V D.C. applied to it by a Hewlett Packard Harrison 6515A D.C. Power Supply.

The light intensity for a particular transition was maximized by observing the photocurrent on a Keithley 150B Microvolt Ammeter and adjusting the wavelength setting of the spectrophotometer to achieve a maximum.

An absorption or fluorescence signal caused the photomultiplier to create a current pulse that in turn created a potential difference across a resistor. In the Mg experiment a 100 kΩ resistor was employed while in the

Ca experiment 10, 22 and 47 kΩ resistors were used. These resistors produced adequate signal to noise ratios without discernably distorting the absorption signal. The resistor was connected in parallel with the input of a Tektronix Type D amplifier. A Tektronix 549 oscilloscope and the input of the Analog-to-Digital Converter of a PDP-LAB8/E computer were connected in parallel to the amplifier output. The oscilloscope was used to display the signals. The Analog-to-Digital Converter sampled the signal voltage once every 50 μsec for Ca and once every 500 μsec for Mg. The voltage and the time were stored in the computer's memory for further processing. The computer began sampling the voltage signal when it was triggered by a Schmidt trigger which was itself triggered by voltage signals of a preset size.

E. Sample Preparation

Cylindrical quartz absorption cells with quartz windows were specially prepared by a glassblower[63] with only one quartz window affixed. The cells were 60.9 cm long and either 2.54 or 5.08 cm in diameter with a piece of 8 mm quartz tubing located 7.62 cm from each end of the absorption cylinder. A piece of 8 mm pyrex tubing was joined to each of the pieces of quartz tubing by means of a quartz to pyrex graded seal. One piece of the pyrex tubing was left open while the other piece had a pyrex break seal affixed to it.

The cell was cleaned with a 5% Hydrofluoric acid solution and rinsed six times with distilled water and then allowed to dry. Tantalum foil[64] was employed to line the inner surface of the absorption tube. The impurities present in this foil are listed in Table 12. Four pieces of the foil, each measuring 16 inches long by 6 inches wide by 0.001 inches thick, were separately rolled lengthwise to form a Ta tube and were inserted into the cleaned quartz cell coaxially so that the seams arising from rolling each piece of Ta over itself alternated from the top to the bottom of the cell. Several pieces of the foil were used to impede the progress of hot metal vapor from the element being investigated from creeping through the seams and attacking the quartz tubing. The glassblower then fused the other quartz window onto the cell. A completely assembled quartz absorption cell containing the Ta foil lining is depicted in Figure 14.

Lifetime determinations were made with no liner of any kind in the absorption cell. The results of these measurements yielded values of the lifetime which were a factor of two times shorter than those obtained from a similar cell lined with Ta. This discrepancy may be attributed to quenching collisions between the excited Mg atoms and the contaminants produced by a reaction between the hot Mg vapor and the quartz absorption cell. Lifetime measurements were also made with absorption cells lined with stainless steel and Molybdenum tubes. The lifetime values ob-

TABLE 12

TYPICAL ANALYSIS IN PARTS PER MILLION OF THE TANTALUM FOIL USED IN THIS WORK

Oxygen	70
Nitrogen	30
Carbon	35
Aluminum	<10
Chromium	< 1
Copper	< 1
Iron	20
Molybdenum	<10
Niobium	<25
Nickel	15
Silicon	13
Titanium	< 5
Tungsten	<40
Tantalum	Balance

FIGURE 14

Quartz Absorption Cell with Tantalum Liner

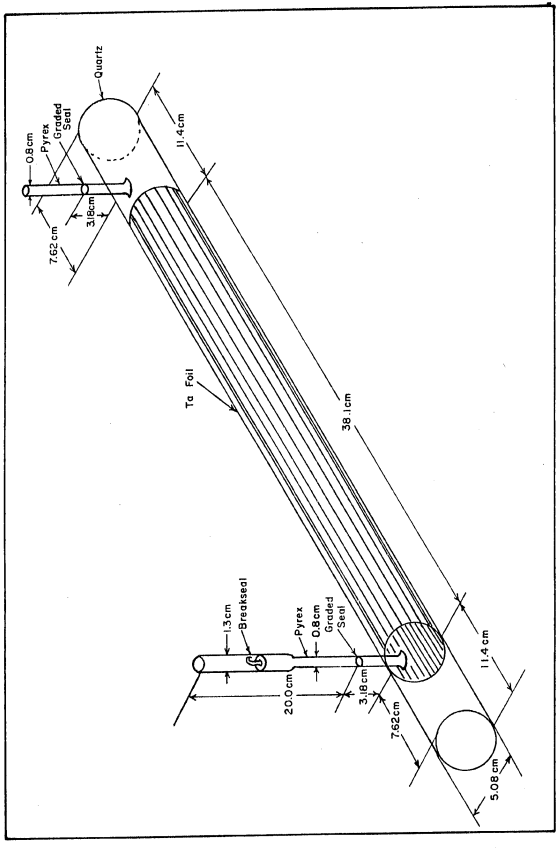

tained from the Molybdenum lined absorption cell were a factor of approximately four times shorter than those obtained from a similar Ta lined cell. The Mo liner was not as clean as the Ta liner. The background pressure only reached a lower limit of 6×10^{-7} Torr even after being heated at 800 ^{o}C for 3 days. Thus, contaminants still present on the Mo surface could have been responsible for the lower lifetime values. The Mo liner also greatly reduced the diameter of the absorption cell. This may have resulted in shorter lifetimes because of the increased probability of quenching collisions between excited Mg atoms and the Mo liner. The measurements with the stainless steel lined sample gave results consistent with those obtained with a Ta lined sample for high values of the buffer gas pressure. However, as the buffer gas pressure was reduced to about 20 Torr a pronounced shortening of the lifetime was observed. The stainless steel liner also reduced the effective diameter of the absorption cell and this made quenching collisions between excited Mg atoms and the cell walls possible at low buffer gas pressures. It was decided that Ta foil was the most suitable lining material because of its resistance to reactions with hot metal vapors, the relative ease with which it could be outgassed to low background pressures and its negligible effect on the effective diameter of the absorption cell.

The sample was attached to a vacuum system with a cold trap in the form of a U-tube between the sample and the

rest of the vacuum system. The vacuum system consisted of a forepump, a turbomolecular pump, high vacuum valves and a capacitive manometer all interconnected by pyrex glass tubing and kovar to pyrex graded seals. The vacuum system is depicted schematically in Figure 15. The sample was attached to the vacuum system at point A shown in the figure. A turbomolecular pump was used in this experiment in order to minimize the risk of contamination of the vacuum system by organic contaminants. The sample was evacuated and all portions of it were outgassed inside of a firebrick oven at a temperature of 450 ^{o}C. The cold trap between the sample and the vacuum system was filled with liquid Nitrogen during the evacuation process. The high vacuum valves were held in their open position by bakeout clamps and the valves, the Bayard-Alpert ion gauge and the interconnecting glassware were baked in a fiberfrax tent at 300 ^{o}C. Heat lamps were used to bake the C valve connecting the turbomolecular pump and the rest of the vacuum system. The capacitive manometer was baked in a seperate fiberfrax tent to 300 ^{o}C while bakeout heaters were used on the turbomolecular pump itself. The remaining exposed glassware was heated by heat tapes or flamed periodically with a bunsen burner. Heat was applied until the background pressure as measured by a Bayard-Alpert ion gauge on the turbomolecular pump side of the C valve was reduced to about 2 x 10^{-5} Torr of Hg. After allowing the components of the vacuum system to cool to room temperature, a pressure of approximately 10^{-7} Torr of Hg was obtained.

FIGURE 15

Schematic diagram of Vacuum - Gas Handling System

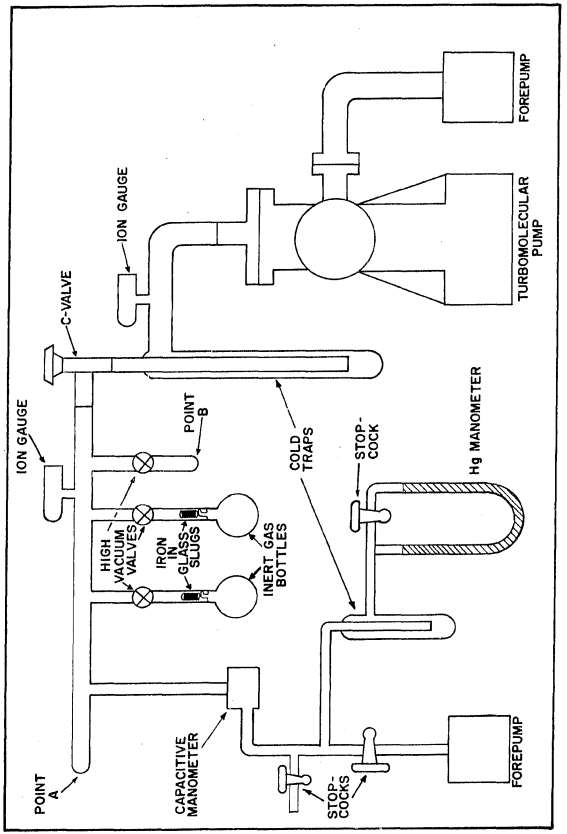

The system was slowly let up to air and the U-tube cold trap was removed. The sample was then reattached to the vacuum system with a piece of Ca or Mg situated halfway between the front window of the cell (i.e., the window near the port without the break seal) and the Ta foil.

A manufacturer's list of the impurities present in the Ca[65] and Mg[65] is given in Table 13. The Ta-lined part of the cell and the rear window were placed inside a fire-brick oven and baked at 700 °C. The other components of the vacuum system were also heated again in the manner described above. The system was heated until the pressure was reduced to 7 x 10^{-5} Torr of Hg at which time the Ca or Mg chunk was outgassed under vacuum by heating the quartz cell wall on which it rested with a bunsen burner until the background pressure began to decrease again. The bakeout of the system continued until a pressure of 5.7 x 10^{-7} Torr was reached at which time only the sample continued to be heated. The piece of Mg or Ca was outgassed once again. Only when the background pressure had decreased to 2 x 10^{-7} Torr of Hg as measured on the ion gauge on the sample side of the C valve with the sample at a temperature of 800 °C was the heat on the sample oven turned off. Upon cooling to room temperature the pressure was determined to be 7 x 10^{-8} Torr of Hg. The sample was then sealed off under vacuum of the pyrex side of the quartz to pyrex graded seal of the non-break seal exit port of the sample. In previous work on Mg by Wright et al.[27] samples were heated at 800 °C until a back-

TABLE 13

TYPICAL IMPURITY LEVELS IN PARTS PER MILLION OF THE CHEMICALS USED IN THIS WORK

Calcium

Magnesium	4000
Aluminum	100
Iron	50
Manganese	30
Others	< 20

Magnesium

Boron	20
Sodium	5
Potassium	5
Silver	20
Silicon	< 10
Calcium	10
Carbon	50
Hydrogen	10
Others	< 5

ground pressure of 2 x 10^{-6} Torr was achieved. Measurements of the lifetime using these samples resulted in a lifetime value 50% shorter than that quoted in this investigation. The sealed-off sample was then placed in an oven on the table supporting the dye laser and the spectophotometer. A slug consisting of a piece of magnetized iron encapsulated in pyrex glass 1.75 inches long and 3/8 of an inch in diameter was placed on top of the sample break seal. The sample was then reattached to the vacuum system by means of the break seal port at point B of the vacuum system as shown in Figure 15. At the same time pyrex bottles of Research Grade Inert Gases[60] with their own break seals and slugs were attached to the vacuum system as shown in Figure 15. The break seals and slugs were cleaned with Hydrofluoric acid solution and rinsed in distilled water before being used on the vacuum system. Table 14 records the impurities present in the inert gases while Table 15 lists the impurities present in the H_2 and N_2 gases used in this work. All possible components of the vacuum system were again baked to outgas their inner surfaces. The bakeout continued until a pressure of 10^{-6} Torr of Hg was attached. With all heat removed from the system, the background pressure of the system was 4.4 x 10^{-8} Torr. The break seal connecting the sample and the system was broken and evacuation of the system continued until a pressure of 4 x 10^{-8} Torr was again attained. The sample was then ready for use.

TABLE 14

TYPICAL ANALYSIS IN PARTS PER MILLION OF THE INERT GASES USED IN THIS WORK

Helium and Argon

Total Hydrocarbons	< 1
Carbon Dioxide	< 1
Hydrogen	< 1
Methane	< 1
Water	< 3
Neon	< 1
Nitrogen	< 2
Oxygen	< 1

Neon

Argon	1
Carbon Dioxide	1
Helium	< 20
Total Hydrocarbons	< 1
Hydrogen	< 1
Krypton	< 1
Methane	< 1
Water	< 3
Nitrogen	< 5
Oxygen	< 1

TABLE 15

TYPICAL ANALYSIS IN PARTS PER MILLION OF THE H_2 AND N_2 GAS USED IN THIS WORK

Hydrogen	
Argon	< 1
Carbon Dioxide	< 1
Helium	< 5
Total Hydrocarbons	< 1
Methane	< 1
Water	< 3
Nitrogen	< 1
Oxygen	< 1

Nitrogen	
Argon	< 20
Carbon Dioxide	< 1
Helium	< 2
Total Hydrocarbons	< 1
Oxygen	< 1
Hydrogen	< 1
Methane	< 1
Water	< 1
Neon	< 3

CHAPTER IV

DATA AND RESULTS

Measurements were made to determine the lifetime of the $^3P_1$ metastable level of Ca and Mg over a wide range of experimental conditions. These studies were undertaken to determine any functional dependence of the lifetime on the experimental variables and also to investigate any possible sources of systematic error in the measurement technique. The experimental data and results for Ca and Mg will be presented separately. A comparison of the Ca and Mg results will be made at the close of this chapter.

A. Calcium

1. Thermal Equilibrium Measurements

In Chapter II a theoretical model for the time dependence of the absorption of light by atoms in the ^3P fine structure levels was derived. A major assumption in this derivation was that the populations of the $^3P_2$, $^3P_1$ and $^3P_0$ levels corresponded to the populations expected under conditions of thermal equilibrium. In particular, the existence of thermal equilibrium was assumed in order to compute β, the fraction of the total population of the ^3P levels in the $^3P_1$ level. This assumption was verified

experimentally. The ratios of the populations of the Ca ^3P fine structure levels were experimentally measured in the manner outlined in section B of Chapter III. These measured ratios were compared to the theoretical ratios. The ratios of the populations of the Ca ^3P levels obtained experimentally fell within 4% of the theoretical estimates of the population ratios. These measurements verified the assumption of thermal equilibrium and confirmed the choice of $\beta = 0.36$ for Ca.

2. Quenching of Metastable Ca Atoms by H_2 and N_2

The next phenomenon to be investigated was the quenching of Ca atoms in the $^3P_1$ level to their ground state by collisions of the second kind with H_2 and N_2 gas. This would result in a shortening of the measured value of the lifetime of the Ca $^3P_1$ level. The energy transferred in these collisions either serves to increase the kinetic energies of the collision partners or to excite the H_2 and N_2 molecules. The processes involved are therefore:

$$X + Ca^* \longrightarrow X + Ca + \text{kinetic energy} \quad (64)$$

or

$$X + Ca^* \longrightarrow X^* + Ca \quad (65),$$

where X is a H_2 or N_2 molecule and * denotes an excited atom or molecule. De-excitation of Ca $^3P_1$ metastable atoms may also occur because of collisions between these atoms and

the walls of the absorption cell at low foreign gas pressures.

Measurements were made to determine the rate of quenching of excited Ca $^3P_1$ atoms by H_2 and N_2 gas. The data was obtained by monitoring the absorption out of the ^3P levels as described in section A of Chapter III. However, the PDP-LAB8/E computer was not used in performing the quenching rate measurements since the maximum rate at which it could sample absorption signals proved to be too slow. The quenching data for Ca was obtained from measurements performed with 2.54 cm diameter absorption cells. Each measurement of the lifetime of the Ca $^3P_1$ level was performed by monitoring the absorption of light out of one of the ^3P levels with a fixed pressure of H_2 or N_2 gas in the absorption cell. A photograph of the trace of the absorption signal displayed on the oscilloscope was then obtained. The absorption signal was fit to a simple exponential function of the form

$$V(t) = A'' \exp(-t/\Gamma) + B \qquad (62),$$

where V(t) is the voltage, A" is the amplitude coefficient, t is the time, Γ is the observed lifetime and B is the D.C. baseline of the light. The voltage, V(t), minus the baseline, B, was read from the photographs as a function of time. These readings were then plotted on semi-log paper yielding a straight line from which the lifetime could be obtained. Data acquisition and analysis proceeded in this

manner for several different pressures of H_2 and N_2 gas.

The relationship between the measured lifetime, τ_m, and the true lifetime, τ, in the presence of a foreign gas is given by[66]

$$1/\tau_m = a + b/P + cP \qquad (66),$$

where a is $1/\tau$, and P is the foreign gas pressure. The term b/P is included to account for quenching of the metastable atoms at the cell walls at low foreign gas pressures. The term cP accounts for quenching of metastable Ca atoms by collisions of the second kind with foreign gas molecules.

A least squares fit to the function

$$1/\tau_m = a + cP \qquad (67)$$

was performed, where the term describing quenching at the cell walls was neglected. This analysis gave total quenching rates of $2.74 \pm 0.18 \times 10^3$ sec^{-1} Torr^{-1} for H_2 and $2.18 \pm 0.47 \times 10^3$ sec^{-1} Torr^{-1} for N_2. A multiple regression analysis was then performed in which a function of the form

$$y = a + bx_1 + cx_2 \qquad (68)$$

was taken as the regression model. In the above formula $y = 1/\tau_m$, $a = 1/\tau$, $x_1 = 1/P$ and $x_2 = P$. This analysis demonstrated that the inclusion of the 1/P diffusion term reduced the sum of the squares of the residuals by a negligible amount in fitting the data. The sum of the squares

of the residuals was reduced from 1.64 to 1.54 for the H_2 data and from 5.41 to 5.40 for the N_2 data. A statistical F test[67] was also performed to see whether or not the additional term improved the value of the sum of the squares of the residuals by a significant amount. This test indicated that there was no significant improvement in the fit with the addition of the 1/P diffusion term. The diffusion term may also be neglected on the basis that its coefficient is so small that a negligible error is introduced by neglecting the term b/P for the range of pressures involved in this experiment.

The respective values of $2.74 \pm 0.18 \times 10^3$ and $2.18 \pm 0.47 \times 10^3$ sec^{-1} $Torr^{-1}$ for the H_2 and N_2 quenching rates serve as indications of the levels of H_2 and N_2 background pressures that can be tolerated without appreciably affecting the lifetime. For example, background pressures on the order of 10^{-2} Torr would introduce less than a 1% error in the lifetime measurements. Measurements of the background pressure as a function of time with the vacuum pump valved off showed that the background pressure did not exceed 10^{-5} Torr during runs in which lifetimes were measured. Therefore, quenching by background contaminants can be neglected.

3. Ca Vapor Pressure and Buffer Gas Pressure Dependence

Experimental investigations were performed to determine the dependence of the lifetime of the Ca $^3P_1$ level on the Ca vapor pressure and the inert buffer gas pressure. The inert buffer gases used were Neon and Argon. Data was taken using both 2.54 and 5.08 cm diameter absorption cells. The lifetime values, obtained from the 2.54 cm diameter cells, were acquired from the computer analysis of a single absorption signal. However the lifetime values obtained from the 5.08 cm diameter absorption cells, were obtained from the analysis of the signal average of 20 absorption signals. All of the measurements were taken with the laser beam expanded.

The buffer gas dependence of the lifetime was investigated by obtaining data with the absorption cell at a constant temperature and hence at a constant vapor pressure. The Ne and Ar gas pressures were varied from 20 to 500 Torr. The results of these lifetime determinations are presented in Figure 16. The mean value of the reciprocal of the lifetime at each buffer gas pressure is plotted versus the buffer gas pressure. The error bars represent the standard error of the mean (i.e., the standard deviation from the mean divided by the square root of the number of measurements).[68] The horizontal line corresponds to the unweighted average of all the measurements independent of the buffer gas pressure.

FIGURE 16

Graph of reciprocal of Ca $^3P_1$ lifetime versus buffer gas pressure. Each point is the mean of several measurements and the error bars represent the standard error of the mean. The horizontal line is the mean of 157 measurements of the reciprocal lifetime. ($1/\tau_{ave}$ = $2.54 \pm 0.02 \times 10^3$ sec^{-1}).

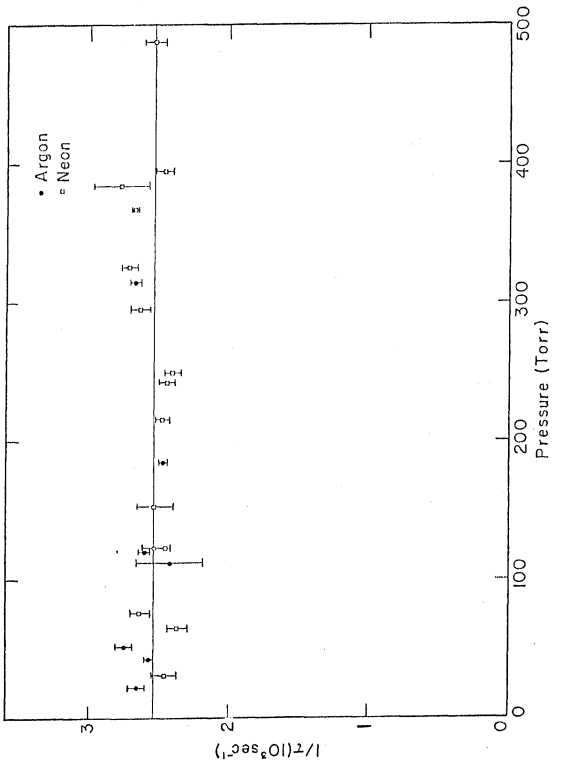

The buffer gas pressure could have affected the lifetime measurements because of the possibility of quenching collisions of the second kind as in the case of quenching by H_2 and N_2 gas. However, quenching collisions are not as likely since Ar and Ne are inert gases. Diffusion of excited Ca atoms to the cell walls at low buffer gas pressures could also have affected the lifetime measurements.

A multiple regression analysis was performed with equation (66) as the fitting function using data obtained at a constant temperature for various values of the Ar or Ne buffer gas pressure. Statistical F tests demonstrated that no significant correlation existed between $1/\tau_m$ and P irrespective of the type of buffer gas and the diameter of the absorption cell used. Statistical F tests also demonstrated that there was no significant correlation between values of $1/\tau_m$ and $1/P$ independent of the type of the buffer gas and the diameter of the absorption cell employed. A least squares fit to the data obtained at a constant temperature was also performed. In this analysis a functional relationship between $1/\tau_m$ and P of the form

$$1/\tau_m = a + cP \tag{67}$$

was assumed. The coefficient c was determined to be approximately 10^{-4} sec^{-1} $Torr^{-1}$. Neglecting the pressure dependence over the range of pressures for which lifetime measurements were made would therefore introduce a negligible

in the value obtained for τ. On the basis of the above analysis, it was concluded that over the range of pressures at which lifetime measurements were made the Ca $^3P_1$ lifetime demonstrated no buffer gas pressure dependence.

The variation of the Ca $^3P_1$ lifetime as a function of the Ca vapor pressure was investigated at several fixed buffer gas pressures. The results of these measurements are presented in Figure 17. The mean value of the reciprocal of the lifetime obtained at a constant value of the Ca vapor pressure is plotted versus the logarithm of the Ca vapor pressure. The error bars represent the standard error of the mean while the horizontal line represents the unweighted average of all lifetime measurements made with the Ca vapor pressure below 0.1 Torr.

The lifetime measurements could have been systematically lengthened by reabsorption of the fluorescence from Ca $^3P_1$ atoms by ground state Ca atoms. This process is sometimes called "radiation trapping" and depends on the density of ground state atoms and hence on the Ca vapor pressure. The lifetime measurements could also have been systematically shortened by quenching collisions between excited $^3P_1$ Ca atoms and ground state Ca atoms. This effect would also depend on the Ca vapor pressure.

The graph of the reciprocal of the Ca $^3P_1$ lifetime versus the logarithm of the Ca vapor pressure shown in Figure 17 exhibits neither a systematic lengthening nor shortening of the lifetime for values of the Ca vapor pressure

FIGURE 17

Graph of reciprocal of Ca $^3P_1$ lifetime versus logarithm of Ca vapor pressure. Each data point is the mean of several measurements and the error bars represent the standard error of the mean. The horizontal line is the mean of 157 measurements of the reciprocal lifetime. ($1/\tau_{ave} = 2.54 \pm 0.02 \times 10^3$ sec^{-1}).

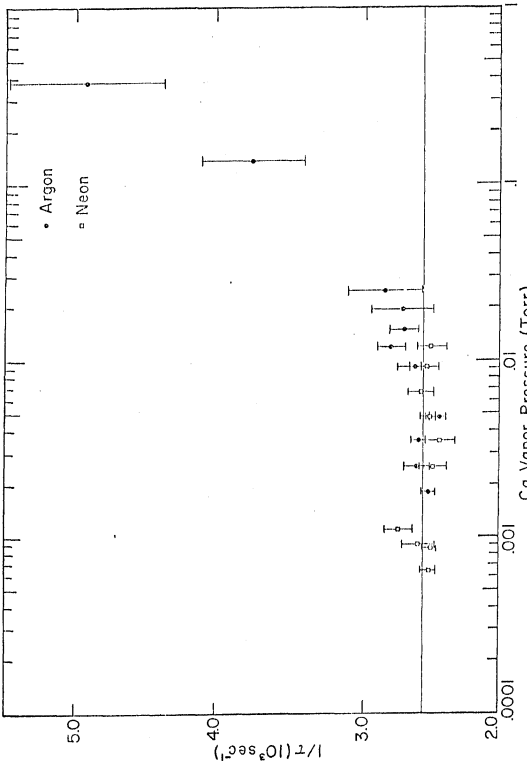

between 10^{-4} and 10^{-1} Torr. One may conclude that the systematic errors introduced by radiation trapping and quenching collisions were either so small as to be negligible or that they were significant but being of opposite signs and the same order of magnitude their effects cancelled.

A paper by Barrat[69] indicates that if radiation trapping is present, the measured lifetime is given by

$$\tau_m = \tau/(1-x) \qquad (69),$$

where τ is the lifetime in the absence of radiation trapping, τ_m is the measured lifetime and x is given by

$$x = 1 - \exp(-(\pi/6)^{1/2} k_0 \ell) \qquad (70).$$

In the expression for x given above, ℓ is the absorption path length and k_0 is defined by equation (9) which is found in Chapter II. The equation for τ_m may be recast in terms of the Ca vapor pressure, P_{vap}, and the absolute temperature, T, as

$$1/\tau_m = 1/\tau - (1 - \exp(-s\ell P_{vap}/T^{3/2}))/\tau \qquad (71),$$

where s is a constant.

The expression for the measured lifetime if quenching collisions are occurring is given by[70]

$$1/\tau_m = 1/\tau + Q P_{vap}/T^{1/2} \qquad (72),$$

where Q is a constant related to the quenching cross section.

Most of the Ca data presented in this work was ob-

tained at T ≈ 850°K and $P_{vap} \simeq 10^{-2}$ Torr. An estimate of the error introduced by the presence of both radiation trapping and collisional quenching may be calculated from the relation

$$1/\tau_m = 1/\tau + 1/\tau_c - 1/\tau_r \qquad (73),$$

where

$$1/\tau_c = Q P_{vap}/T^{1/2} \qquad (74)$$

and

$$1/\tau_r = (1 - \exp(-s\ell P_{vap}/T^{3/2})) \qquad (75).$$

Using realistic estimates of the parameters involved, a calculation of the amount of error introduced by the joint effect of radiation trapping and collisional quenching yields a value of 5% error in the lifetime determinations. This amount of variation would not have been discerned during lifetime measurements.

A least squares fit to the equation

$$1/\tau_m = a + c P_{vap} \qquad (76)$$

was made using lifetime data obtained at constant buffer gas pressures. This analysis indicated that the inclusion of the term cP_{vap} changed the value obtained for τ by 1%, for vapor pressures less than 10^{-1} Torr. Statistical F tests also indicated that there was no significant correlation between the reciprocal of the lifetime and the Ca

vapor pressure.

The lifetime of the Ca $^3P_1$ level is shortened for vapor pressures above 10^{-1} Torr as indicated in Figure 17. This effect may be due to quenching collisions between excited and non-excited Ca atoms. However, this effect was most probably caused by quenching collisions between Ca atoms and contaminants driven off the inner surface of the Ta liner and the absorption tube at high temperatures. On the basis of the above analysis it was concluded that for Ca vapor pressures between 10^{-4} and 10^{-1} Torr, the lifetime of the Ca $^3P_1$ level did not depend on the Ca vapor pressure.

4. Ca Results

The lifetime of the Ca $^3P_1$ level displayed no strong buffer gas or vapor pressure dependence for buffer gas pressures from 20 to 500 Torr and vapor pressures less than 10^{-1} Torr as indicated in the last section. The unweighted average of all the measurements in the aforesaid vapor pressure and buffer gas pressure ranges was therefore taken as the experimental value for the lifetime of the $^3P_1$ metastable level. The mean of 157 measurements of τ is 0.393 ± 0.003 msec. The quoted error is a measure of the random error in the average value of τ. The error corresponds to the standard error of the mean of 157 measurements. A histogram showing the distribution of the experimental values of τ is presented in Figure 18. Superimposed on the histogram is a plot of the function $kf(\tau)\Delta\tau$ versus τ. This

FIGURE 18

Histogram of Ca $^3P_1$ lifetime values. Superimposed on the histogram is a plot of the function $kf(\tau)\Delta\tau$ versus τ. This function is the probability that a value of τ will lie within an interval of width $\Delta\tau$ if k measurements of τ are made.

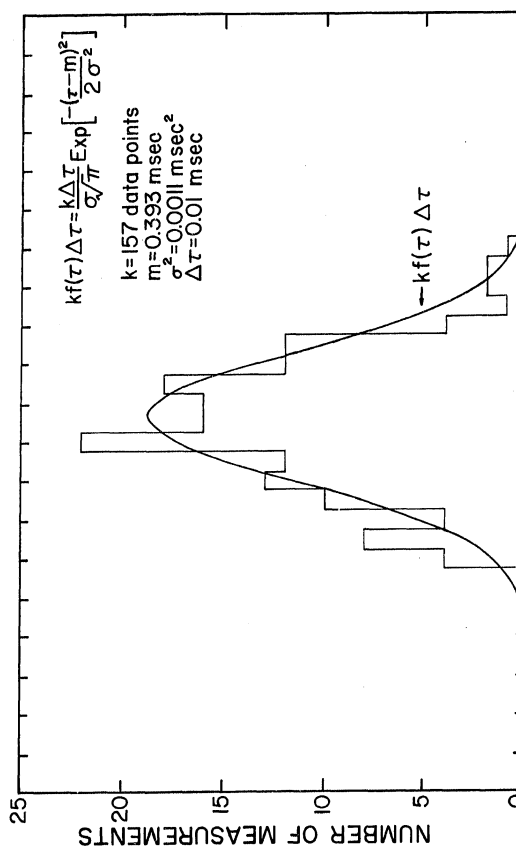

function is the probability that a value of τ will lie within an interval of width $\Delta\tau$ if k measurements of τ are made. We assumed that there was a distribution of values of τ due to random measurement errors and we assumed that the distribution function of the τ values, $f(\tau)$, was Gaussian.

In addition to the random error quoted above, estimates of the systematic error in the Ca measurements must also be made. Several sources of systematic error will now be considered. There was no significant difference observed between lifetimes measured in the 2.54 cm versus the 5.08 cm diameter absorption cells. Therefore, one may conclude that quenching of the metastables by collisions with the walls of the absorption cell was not a significant problem even at low buffer gas pressures.

The effect of quenching collisions between metastable atoms and the inert buffer gas atoms was investigated by changing the buffer gas pressure by an order of magnitude during lifetime measurements. No significant effect was observed.

Measurements were made in which the intensity and degree of self-reversal of the radio frequency discharge lamp was varied. These variations produced no significant change in the measured value of the lifetime. The time base of the Analog-to-Digital Converter was checked and found to be operating properly. An exponentially decaying pulse of known time constant was produced by discharging a capacitor through a resistor. This pulse was analyzed by

the computer and the time constant obtained from this analysis was in excellent agreement with the RC time constant of the circuit. This test indicated that no large systematic error due to an electronic malfunction was present. The linearity of the photomultiplier tube was also checked and found to be adequate. The process of quenching by ions produced by photo-ionization may be neglected since this would require the absorption of three photons, which is not likely to occur.

Radiation trapping and quenching due to Ca-Ca collisions would depend on the Ca vapor pressure. The Ca vapor pressure was varied from approximately 10^{-4} to 10^{-1} Torr. The measured lifetime values did not change by any significant amount. At vapor pressures above 10^{-1}Torr, however, the lifetime was significantly shortened. This shortening of the lifetime could be explained either in terms of Ca-Ca quenching collisions or in terms of the outgassing of residual contaminants from the Ta liner. None of the lifetime data obtained at vapor pressures above 10^{-1} Torr was included in the calculations of the final lifetime value quoted in this work.

If the radiation from the laser was sufficiently intense the population of the $^3P_1$ level could have been large enough to have resulted in the absorption of more than 20% of the incident light from the R.F. discharge lamp. In Chapter II it was shown that for small absorption signals the simple exponential and the exponential to an exponential

absorption models agreed well with the more exact integral absorption expression. An analysis similar to that depicted in Figure 6 of Chapter II indicates that if the amount of absorption was 25% an error of approximately 0.040 msec in the lifetime value would have resulted. Although care was taken to avoid this difficulty by only analyzing small absorption signals, variations of the lifetime with the laser power were observed from time to time. If the above estimate of the systematic error is combined in quadrature with the random error, the uncertainty in the measured lifetime becomes 0.040 msec. Therefore, the final result and uncertainty quoted in this investigation for the Ca $^3P_1$ lifetime is 0.393 $\pm$ 0.040 msec.

B. Magnesium

1. Thermal Equilibrium Measurements

Measurements were performed to test the hypothesis that the populations of the Mg ^3P fine structure levels conformed to the populations predicted for thermal equilibrium. Measurements of the ratios of the populations of the Mg ^3P levels were performed by Wright et al.[27] Their work indicated that the theoretical and experimental values for the Mg ^3P population ratios agreed to within 2%. Corroborative measurements were also made during the course of this work which yielded comparable results. These measurements confirmed the choice of β = 0.34 for Mg and verified

the assumption of thermal equilibrium used in this work.

2. Quenching of Metastable Mg Atoms by H_2 and N_2

The next phenomenon to be investigated was the quenching of Mg atoms in the $^3P_1$ level to their ground state by collisions of the second kind with H_2 and N_2 gas. Measurements of the quenching rates were made by Wright et al.[27] Their data is graphically displayed in Figure 19. Their values for the quenching rates were 1.1×10^4 sec^{-1} $Torr^{-1}$ for H_2 and 4.4×10^3 sec^{-1} $Torr^{-1}$ for N_2. These values indicate the levels of H_2 and N_2 background pressures that can be tolerated without significantly affecting the lifetime of the Mg $^3P_1$ level. For example, background pressures of H_2 and N_2 below 10^{-5} Torr would have no significant effect on the observed lifetime. Measurements of the background pressure as a function of time with the vacuum pump valved off showed that the background pressure did not exceed 10^{-6} Torr during runs in which the lifetime was measured. Therefore, quenching by background contaminants can also be neglected in the Mg experiments.

3. Mg Vapor Pressure and Buffer Gas Pressure Dependence

Measurements were made to determine the dependence of the lifetime of the Mg $^3P_1$ level on the Mg vapor pressure and the inert buffer gas pressure present in the absorption cell. The inert buffer gases used were He, Ne and Ar.

FIGURE 19

Graph of reciprocal of Mg $^3P_1$ lifetime versus H_2 and N_2 gas pressure.

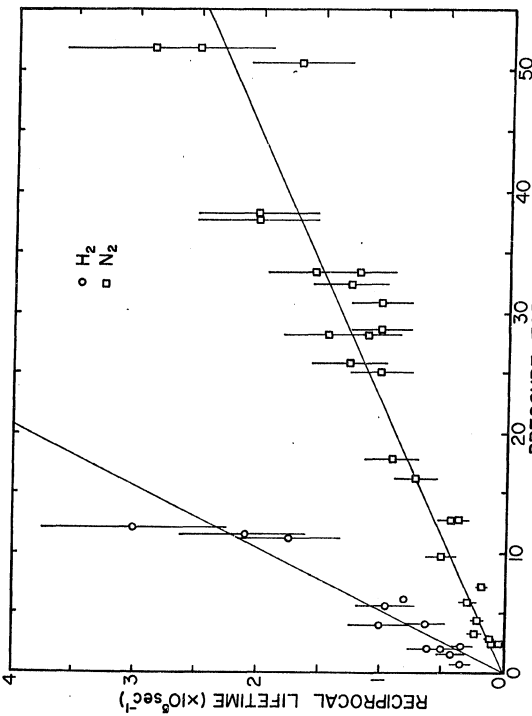

These measurements were performed with 5.08 cm diameter absorption cells in order to minimize the possibility of quenching collisions between excited Mg atoms and the walls of the absorption cells. Data was obtained with the laser beam expanded and unexpanded. Each of the absorption signals analyzed was the signal average of from 10 to 20 individual absorption signals.

Measurements were conducted in which the temperature of the absorption cell was varied while the buffer gas pressure was held constant. This was done in order to ascertain whether or not the lifetime of the $^3P_1$ level of Mg was affected by variations in the Mg vapor pressure. Statistical F tests showed that there was no significant correlation between $1/\tau$ and the Mg vapor pressure. Thus, there was no indication of the presence of radiation trapping or Mg-Mg collisional quenching.

Determinations of the lifetime were also made in which the Mg vapor pressure was held constant while the buffer gas pressure was varied over a 500 Torr pressure range. The lifetime, τ, was observed to have been appreciably shortened at low values of the buffer gas pressure.

The lifetime data was analyzed by performing a least squares fit of the data to a function of the form

$$1/\tau_m = a + b/P \qquad (77),$$

where τ_m is the measured lifetime, a is $1/\tau$ at infinite buffer gas pressure and P is the buffer gas pressure. A

statistical F test indicates that a correlation exists between the variables $1/\tau_m$ and $1/P$ at the 99% level of confidence, for each of the three buffer gases used. A multiple regression analysis was performed using the model

$$y = a + bx_1 + cx_2 \tag{68}$$

in which $y = 1/\tau$, $x_1 = 1/P$ and $x_2 = P$. This analysis demonstrated that the inclusion of the buffer gas quenching term, cx_2, reduced the sum of the squares of the residuals by a negligible amount (from 0.18×10^{-2} to 0.15×10^{-2} for He, from 0.38×10^{-3} to 0.26×10^{-3} for Ne and from 0.607×10^{-3} to 0.601×10^{-3} for Ar). Statistical F tests also indicated that there was no significant improvement in the fit with the inclusion of the buffer gas quenching term. Thus, the lifetime of the Mg $^3P_1$ level was significantly affected by quenching of the metastables at the cell walls at low buffer gas pressures. However, quenching of metastable Mg atoms to their ground state by collisions of the second kind with the inert buffer gas atoms was not a significant effect. The absence of collisional quenching by the buffer gas atoms also indicates that no significant amount of contamination was entering the absorption sample with the buffer gas since the amount of contamination introduced would be directly proportional to the buffer gas pressure.

4. Mg Results

The results of the above analysis indicate that radiation trapping and Mg-Mg quenching collisions were not significant factors affecting the lifetime of the Mg $^3P_1$ level. There was also no indication of quenching by the inert buffer gas atoms. However, diffusion of the metastables and their subsequent de-excitation at the walls of the cell was clearly evident.

The results of the measurements of the lifetime as a function of the buffer gas pressure are presented in Figures 20 and 21. In these figures each data point represents the average value of the reciprocal of the lifetime at a given buffer gas pressure. The error bars represent the total error due to both random and systematic errors. The magnitude of the systematic error in the Mg $^3P_1$ lifetime determinations was estimated in the same manner as the systematic error in the Ca lifetime determinations. In Figure 21 the lifetime values obtained at 11, 13 and 452 Torr of Ar are of questionable value. Therefore, although they are shown for completeness, they were not included in the least squares fit to determine the Mg $^3P_1$ lifetime. The smooth curves drawn through the data points in both figures represent the least squares fit of the data to the function

$$1/\tau_m = a + b/P \qquad (77).$$

FIGURE 20

Graph of reciprocal of Mg $^3P_1$ lifetime versus He and Ne buffer gas pressure. The error bars represent the total error due to both random and systematic errors.

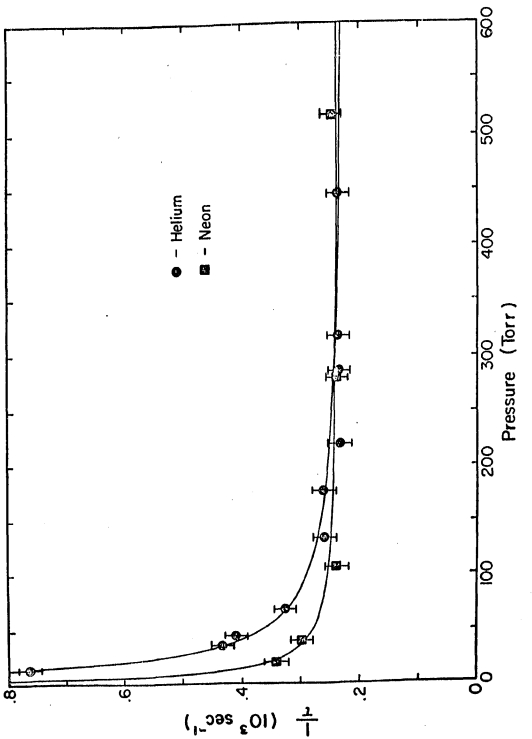

FIGURE 21

Graph of reciprocal of $Mg\ ^3P_1$ lifetime versus Ar buffer gas pressure. The error bars represent the total error due to both random and systematic errors.

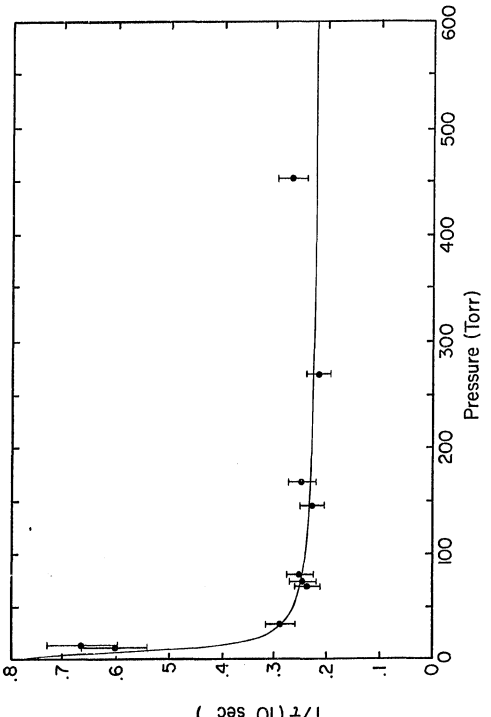

Extrapolation was made to infinite buffer gas pressure in order to obtain the lifetime. The extrapolated lifetime values for He, Ne and Ar are 4.65 ± 0.51, 4.35 ± 0.51 and 4.62 ± 0.53 msec respectively. The error quoted in each instance includes both the error in the fit and an estimate of the systematic error. Taking the average of the above values of the lifetime and combining their errors in quadrature yields the value of 4.54 ± 0.30 msec for the lifetime of the Mg $^3P_1$ level.

In order to check for possible systematic errors inherent in the absorption monitoring technique (e.g., nonlinear absorption) in some runs the decay of metastables was monitored by observing the fluorescence from the $^3P_1$ level. The fluorescence measurements were in substantial agreement with the absorption measurements. The same tests of the proper functioning of the experimental apparatus as performed in the Ca experiment were repeated in the Mg experiment.

C. Comparison of Ca and Mg Results

The lifetime of the Ca $^3P_1$ level was not affected by quenching collisions at the walls of the absorption cell even at low buffer gas pressures. However, the lifetime of the Mg $^3P_1$ level was affected by the de-excitation of metastable atoms at the walls of the absorption cell. This effect was only significant at low values of the buffer gas pressure. In addition, the Mg lifetime measurements were

affected more by the presence of contaminants than were the Ca lifetime measurements. For example, a background pressure of 10^{-2} Torr of H_2 or N_2 could be tolerated in the Ca experiments with only a negligible effect on the lifetime measurements while a much lower pressure (10^{-5} Torr) was necessary in the Mg experiments. Both of these effects can be explained on the basis of the following arguments.

The lifetime of Ca atoms in the $^3P_1$ level is a factor of ten times shorter than that of the Mg atoms in the $^3P_1$ level. Calcium also has an atomic mass that is approximately twice as large as that of Mg. Therefore, Ca atoms would diffuse more slowly to the cell walls than would Mg atoms. The Ca atoms would be more likely than the Mg atoms to have already decayed back to their ground state at the time when collisions with the cell walls occurred. Estimates of the average distance a Ca and Mg atom would diffuse during their lifetimes[73] confirm these suppositions. With a buffer gas pressure of 25 Torr of He in an absorption cell of radius 2.54 cm, Ca atoms would diffuse 0.13 cm in one Ca $^3P_1$ lifetime while Mg atoms would diffuse 0.53 cm in one Mg $^3P_1$ lifetime. In 5 Mg lifetimes excited Mg atoms would diffuse to the cell walls and be quenched while excited Ca atoms would take approximately 20 Ca lifetimes to reach the cell walls.

The fact that Ca has a shorter lifetime than Mg makes it less susceptible to quenching effects. Therefore,

a disagreement between the value obtained in this work for the Ca $^3P_1$ lifetime and the values obtained in other theoretical and experimental work would indicate the presence of systematic errors in our measurement technique. However, no significant disagreement was observed.

CHAPTER V

CONCLUSIONS

A. Discussion of Results

An experimental method for measuring the lifetime of the $^3P_1$ level of Group II atoms was devised and tested. The resulting lifetime measurements may be used to calculate absolute values of the oscillator strengths of the transition $^3P_1 \leftrightarrow {}^1S_0$ for the alkaline earth elements. The method was employed in this investigation to measure the lifetime of the $^3P_1$ level of Ca and Mg.

The lifetime of the Ca $^3P_1$ level is reasonably well known from other experimental work which employed measurement techniques different from those used in this investigation. However, most of these values are the result of relative rather than absolute measurements. A comparison of recent theoretical and experimental determinations of the Ca $^3P_1$ lifetime is presented in Table 16. The results of this investigation agree satisfactorily with the other determinations of the Ca $^3P_1$ lifetime.

The satisfactory agreement between the results obtained in this investigation and the results of other experimental and theoretical work indicates that no large

TABLE 16

SUMMARY OF RECENT THEORETICAL AND EXPERIMENTAL VALUES OF THE Ca $^3P_1$ LIFETIME

AUTHOR	THEORY τ(msec)	EXPT τ(msec)
Luc-Koenig[12] (1974)	0.34	
Victor[13] (1975)	0.34	
Ostrovskii and Penkin[17] (1961)		0.39[a]
Penkin[18] (1964)		0.44
NBS Tables[19] (1969) (weighted average)		0.37 $\pm$ 0.19
This Work[20]		0.393 $\pm$ 0.040

[a]Measured relative to the $^1S_0 \leftrightarrow {}^1P_1$ transition.

sources of systematic error were present in the experimental design. The successful testing of the experimental method was followed by measurements of the lifetime of the Mg $^3P_1$ level.

As indicated in Chapter I, there has been a long standing discrepancy between the results of the theoretical and experimental determinations of the Mg $^3P_1$ lifetime. The experimental method used to determine lifetimes in this work was first employed by Wright et al.[27] to determine the lifetime of the Mg $^3P_1$ level. Unfortunately, their results did not resolve the discrepancy between the theoretical and experimental lifetime values previously obtained. It is now believed that their lifetime value was systematically shortened by quenching collisions between the excited Mg atoms and unknown contaminants in their absorption cells.[30] Since the validity of the experimental technique was verified by the Ca measurements, which are less susceptible to quenching effects, a remeasurement of the Mg $^3P_1$ lifetime was undertaken with greater attention given to sample preparation. The results of recent theoretical and experimental determinations of this lifetime as well as the value obtained in this work are presented in Table 17. The value quoted for the lifetime of the Mg $^3P_1$ level should be viewed as a lower limit because of experimental limitations in independently monitoring the level of comtamination present in the absorption cell. However, this value of the Mg $^3P_1$ lifetime is in substantial agreement with theoretical

TABLE 17

SUMMARY OF RECENT THEORETICAL AND EXPERIMENTAL VALUES OF THE Mg $^3P_1$ LIFETIME

AUTHOR	THEORY τ(msec)	EXPT τ(msec)
Garstang[23] (1962)	4.2	
Laughlin and Victor[24] (1974)	4.6	
Boldt[25] (1958)		1.9 $\pm$ 0.4
NBS Tables[26] (1969) (weighted average)		2.3 $\pm$ 1.2
Wright et al.[27] (1974)		2.2 $\pm$ 0.2
Strumia et al.[28] (1974)		1.8 $\pm$ 0.2
Mitchell[29] (1975)		3.8 $\pm$ 1.2[a]
This Work[30]		4.54 $\pm$ 0.30

[a]Measured relative to the Mg $^1S_0 \leftrightarrow {}^1P_1$ transition.

calculations.

B. Suggestions for Further Study

The experimental methods used in this work might be used with suitable modification to determine the lifetime of the $^3P_1$ level in other atoms in Group II of the periodic table, such as Strontium and Barium. These measurements would permit the determination of absolute transition probabilities and oscillator strengths to be deduced for the $^3P_1 \leftrightarrow {}^1S_0$ transition in these elements.

Studies were made in this investigation of the rate of quenching of metastable Mg and Ca atoms in the $^3P_1$ level to their ground state by means of collisions with H_2 and N_2 atoms. Further studies of quenching collisions of the second kind between metastable alkaline earth atoms and other molecular buffer gases might also be undertaken.

REFERENCES

[1]H. Hubenet, "Abundance determinations in stellar spectra," in Proc. IAU Symp. No. 26, Utrecht, 1964, ed. by H. Hubenet (Academic Press, London, 1966).

[2]H. R. Griem, Plasma Spectroscopy (McGraw-Hill Book Company, Inc., New York, 1964).

[3]E. Hinnov, J. Opt. Soc. Am. 56, 1179 (1966).

[4]J. M. Vaugham, Phys. Rev. 166, 13 (1968).

[5]D. A. Parkes, L. F. Keyser and F. Kaufman, Astrophys. J. 149, 217 (1967).

[6]D. E. Billings, A Guide to the Solar Corona, (Academic Press, New York, 1966).

[7]R. H. Munro, A. K. Dupree and G. L. Withbroe, Solar Phys. 19, 347 (1971).

[8]F. Strumia, Metrologia 8, 85 (1972).

[9]G. W. King and J. H. Van Vleck, Phys. Rev. 56, 464 (1939).

[10]L. A. Vainshtein and I. A. Poluektov, Opt. Spectrosc. 12, 254 (1962).

[11]B. Warner, Mon. Not. R. Astron. Soc. 140, 53 (1968).

[12]Luc-Koenig, J. Phys. 7B, 1052 (1974).

[13]G. Victor, Center for Astrophysics, Cambridge, Massachusetts, Private Communication.

[14]V. K. Prokofjew, Z. Phys. 50, 701 (1928).

[15]J. W. Schuttevaer, M. J. Debont and Th. H. Van Den Broek, Physica 10, 544 (1943).

[16]K. H. Olsen, P. M. Routly and R. B. King, Astrophys. J. 130, 688 (1959).

[17]Yu. I. Ostrovskii and N. P. Penkin, Opt. Spectrosc. 10, 219 (1961).

[18]N. P. Penkin, J. Quant. Spectrosc. Radiat. Transfer 4, 41 (1964).

[19]N.B.S. Tables, W. L. Wiese, M. W. Smith and B. M. Miles, Atomic Transition Probabilities, NSRDS-NBS-22 (U.S. GPO, Washington, D. C., 1969) Vol. II, p. 25.

[20]P. S. Furcinitti, J. J. Wright and L. C. Balling, Phys. Lett. 53A, 75 (1975).

[21]J. G. Frayne, Phys. Rev. 34, 590 (1929).

[22]P. J. Rubenstein, Phys. Rev. 58, 1007 (1940).

[23]R. H. Garstang, J. Opt. Soc. Am. 52, 845 (1962).

[24]C. Laughlin and G. A. Victor, Astrophys. J. 192, 551 (1974).

[25]G. Boldt, Z. Phys. 150, 205 (1958).

[26]N.B.S. Tables, Wiese, Smith and Miles, p.248.

[27]J. J. Wright, J. F. Dawson and L. C. Balling, Phys. Rev. 9A, 83 (1974).

[28]F. Strumia, P. Minguzzi, G. Ginstredi and M. Tonelli, Proceedings of the 4'th International Conference on Atomic Physics, Heidelberg, p. 200 (1974).

[29]C. J. Mitchell, J. Phys. 8B, 25 (1975).

[30]P. S. Furcinitti, J. J. Wright and L. C. Balling, Phys. Rev. 12A, 1123 (1975).

[31]E. W. Foster, Rep. Prog. Phys. 27, 469 (1964).

[32]A. C. G. Mitchell and M. W. Zemansky, Resonance Radiation and Excited Atoms, (Cambridge University Press, London, 1934) pp.92-151.

[33]W. L. Wiese, "Transition Probabilities for allowed and Forbidden Lines, Lifetimes of Excited States," in Methods of Experimental Physics, ed. by B. Bederson and W. L. Fite (Academic Press, New York, 1968), Vol. 7 Part A, p.117.

[34]T. J. McIlrath, Appl. Phys. Lett. 15, 41 (1969).

[35]T. J. McIlrath and J. L. Carlsten, J. Phys. 6B, 697 (1973).

[36]T. Asada, R. Ladenburg and W. Tietze, Phys. Z. 29, 54 (1928).

[37]M. Mizushima, Quantum Mechanics of Atomic Spectra and Atomic Structure, (W. A. Benjamin, Inc., New York, 1970) pp. 289-292.

[38]D. Layzer and R. H. Garstang, Ann. Rev. Astron. Astrophys. 6, 449 (1968).

[39]H. Nussbaum, J. Phys. 7B, 1052 (1974).

[40]Mitchell and Zemansky, op. cit., pp. 92-151 and 165.

[41]R. Loudon, The Quantum Theory of Light, (Clarendon Press, Oxford, 1973) pp. 22-23.

[42]Mitchell and Zemansky, op. cit., p. 118

[43]Ibid., p. 118.

[44]Loudon, op. cit., p. 32.

[45]Mitchell and Zemansky, op. cit., p.115.

[46]Ibid., p. 100.

[47]Ibid., p. 99.

[48]T. J. McIlrath and J. L. Carlsten, Phys. Rev. 6A, 1091 (1972).

[49]S. Chapman and T. G. Cowling, The Mathematical Theory of Non-Uniform Gases, 3rd. ed. (Cambridge University Press, Cambridge, England, 1970).

[50]Mitchell and Zemansky, op. cit., p. 99.

[51]V. Weisskopf and E. Wigner, Z. Phys. 63, 54 (1930).

[52]MItchell and Zemansky, op. cit., p. 160.

[53]Ibid., p. 101.

[54]Ibid., p. 121.

[55]Ibid., p. 323.

[56]JILA REPORT NO. 24, D. Hummer, "The Voigt Function: An Eight-Significant-Figure Table and Generating Procedure," (Joint Institute for Laboratory Astrophysics, Boulder, Colorado, 1964).

[57]DL-32 flashlamp pumped dye laser purchased from Phase-R Corporation, New Durham, New Hampshire 03855.

[58]Laser dyes available from Eastman Organic Chemicals, Eastman Kodak Company, Rochester, New York 14650.

[59]Johns-Manville JM-23 firebricks purchased from Refractories and Building Specialties, Inc., 767 Concord Avenue, Cambridge, Massachusetts 02138.

[60]Linde Specialty Gases purchased from Welders Supply Company, Inc., 128 Wheeler Road, Burlington, Massachusetts 01803.

[61]Mirrors purchased from Oriel Corporation of America, 15 Market Street, Stamford, Connecticut 06902.

[62]Fiberfrax insulation purchased from Carborundum, Electronics Division, Niagara Falls, New York 14302.

[63]Anderson Glass Company, Old Turnpike Road, Fitzwilliams, New Hampshire 03447.

[64]Tantalum foil purchased from Norton Company, Metals Division, 45 Industrial Place, Newton, Massachusetts 02164.

[65]Calcium and Magnesium purchased from Ventron Corporation, Alpha Products, Beverly, Massachusetts 01915.

[66]J. Pitre, K. Hammond and L. Krause, Phys. Rev. 6A, 2101 (1972).

[67]P. R. Bevington, Data Reduction and Error Analysis for the Physical Sciences, (McGraw-Hill Book Company, Inc., New York, 1969) pp. 195-201.

[68]Y. Beers, Introduction to the Theory of Errors, (Addison-Wesley Publishing Company, Inc., Reading, Massachusetts, 1953) pp. 29-31.

[69]J. P. Barrat, J. Phys. Radium 20, 541, 633 and 657 (1959).

[70]Mitchell and Zemansky, op. cit., p. 187.

[71]Beers, op. cit., p. 17.

[72]Ibid., pp. 28-29.

[73]N. Davidson, Statistical Mechanics, (McGraw-Hill Book Company, Inc. New York, 1962) p. 284.

[74]Mitchell and Zemansky, op. cit., p. 94.

APPENDIX I

This appendix will investigate the posibility of altering the time dependence of the ^3P population due to the absorption of light by atoms in the ^3P system. The ^3P system is composed of 3 fine structure P levels. The energy difference between these levels is not large as was shown in Table 3. Furthermore, the populations of the 3 fine structure levels are assumed to be in thermal equilibrium. It would not be unreasonable, therefore, to regard the $^3P_2$, $^3P_1$ and $^3P_0$ levels as just one level denoted by ^3P. The multiplicity or statistical weight, g, of this level is 9.

The absorption of light by atoms in the ^3P level may now be explored. As an example, consider the case of absorption of light corresponding to the transitions $^3P \leftrightarrow {}^3S_1$. The relevant energy level diagram is shown in Figure 22.

Let N_2, N_1 and N_0 be the populations of the $^3S_1$, ^3P and $^1S_0$ levels respectively. The probability for spontaneous decay from the ^3P to the $^1S_0$ level is given by A_{10} while the probability for spontaneous emission from the $^3S_1$ to the ^3P level is given by A_{21}. The rate of stimulated emission from the $^3S_1$ to the ^3P level is given by $B_{21}\bar{W}$. In this context B_{21} is the Einstein B coefficient and $\bar{W}$ is the energy density per unit frequency. The rate of absorp-

FIGURE 22

Energy level diagram for light absorption by ^3P level atoms.

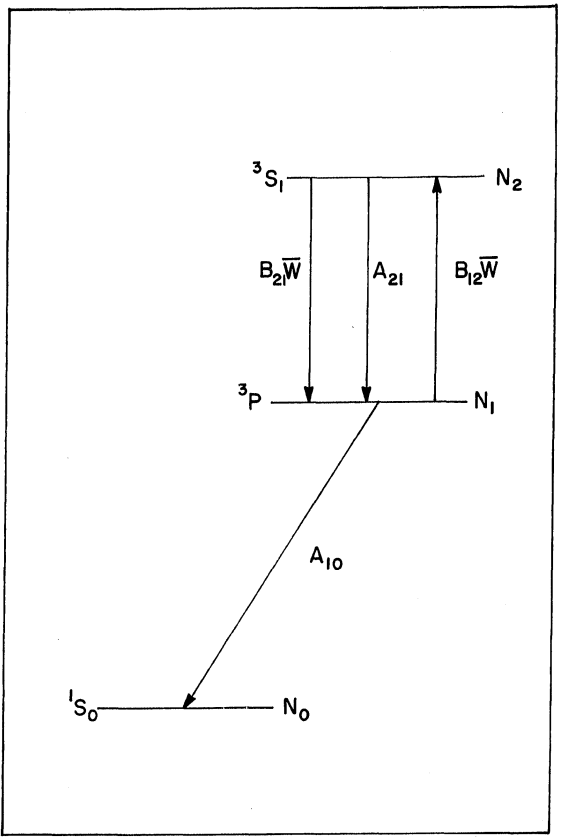

tion of light by atoms in the ^3P level which make the transition to the $^3S_1$ level is given by $B_{12}\overline{W}$. The B coefficients for stimulated emission and absorption of radiation are related by the expression[74]

$$g_1 B_{12} = g_2 B_{21} \tag{78},$$

where g_1 and g_2 are the statistical weights of the ^3P and $^3S_1$ levels respectively. In our case, $g_1 = 9$ and $g_2 = 3$. At time, $t = 0$, the dye laser has produced a population $N_1(0)$ in the ^3P system. The assumption is made that after this time only a negligible amount of radiation of the frequency corresponding to the transition $^3P_1 \leftrightarrow {}^1S_0$ is present to produce stimulated emission or absorption of radiation between the ^3P level and the ground state. The rate equation for the populations of the energy level system depicted above are thus

$$dN_2/dt = B_{12}\overline{W}N_1 - (A_{21} + 3B_{12}\overline{W})N_2 \tag{79},$$

$$dN_1/dt = -(B_{12}\overline{W} + \beta A_{10})N_1 + (A_{21} + 3B_{12}\overline{W})N_2 \tag{80}$$

and

$$dN_0/dt = \beta A_{10} N_1 \tag{81},$$

where the fact that $B_{21} = 3B_{12}$ has been used. Equation (80) may be solved for N_2. The equation for N_2 then becomes

$$N_2 = (dN_1/dt + (B_{12}\overline{W} + \beta A_{10})N_1)/(A_{21} + 3B_{12}\overline{W}) \quad (82).$$

This equation for N_2 may be substituted into equation (79) which becomes

$$dN_2/dt = -\beta A_{10} N_1 - dN_1/dt \quad (83).$$

If the time derivative of equation (80) is taken, the following equation is obtained

$$d^2N_1/dt^2 = -(B_{12}\overline{W} + \beta A_{10})\, dN_1/dt + (A_{21} + 3B_{12}\overline{W})\, dN_2/dt \quad (84).$$

If equation (83) is substituted for dN_2/dt in equation (84) then an equation totally in terms of $N_1(t)$ and its time derivative results. This equation is

$$d^2N_1/dt^2 + (4B_{12}\overline{W} + \beta A_{10} + A_{21})\, dN_1/dt - ((A_{21} + 3B_{12}\overline{W})\beta A_{10})N_1 = 0 \quad (85).$$

This equation has a solution of the form

$$N_1(t) = \int \exp(\lambda_+ t) + \xi \exp(\lambda_- t) \quad (86)$$

in which

$$\lambda_\pm = -(4B_{12}\overline{W} + \beta A_{10} + A_{21})/2 \pm \frac{1}{2}\{(4B_{12}\overline{W} + \beta A_{10} + A_{21})^2 - 4(\beta A_{10}(A_{21} + 3B_{12}\overline{W}))\}^{1/2} \quad (87).$$

After some algebraic manipulation $\lambda\pm$ becomes

$$\lambda_\pm = -(4B_{12}\overline{W} + \beta A_{10} + A_{21})/2 \pm \frac{1}{2}A_{21}\left\{1 + \frac{16B_{12}^2\overline{W}^2}{A_{21}^2} + \frac{\beta^2 A_{10}^2}{A_{21}^2} + \frac{8B_{12}\overline{W}A_{21}}{A_{21}^2} - \frac{4B_{12}\overline{W}A_{10}\beta}{A_{21}^2} - \frac{2\beta A_{10}A_{21}}{A_{21}^2}\right\}^{1/2} \quad (88).$$

Since $A_{21} \simeq 10^8$ sec^{-1}, $\beta A_{10} \simeq 10^3$ sec^{-1} (for Ca, for Mg $\beta A_{10} \simeq 10^2$ sec^{-1}) and $B_{12}\overline{W} \simeq 10^5$ sec^{-1} (upper limit for convential spectroscopic light sources), the above equation may be simplified by neglecting second order terms in $B_{12}\overline{W}$, A_{10} and the product, $A_{10}B_{12}\overline{W}$, when these terms are divided by A_{21}^2.

This simplification results in $\lambda\pm$ being given by the expression

$$\lambda_{\pm} \simeq -\tfrac{1}{2}(4B_{12}\overline{W} + \beta A_{10} + A_{21}) \pm A_{21}\left(1 + \frac{4B_{12}\overline{W}}{A_{21}} - \frac{\beta A_{10}}{A_{21}}\right) \qquad (89).$$

where a binomial expansion of the square root has been made. Therefore,

$$\lambda_{+} \simeq -\beta A_{10} \qquad (90)$$

and

$$\lambda_{-} \simeq -(A_{21} + 4B_{12}\overline{W}) \qquad (91)$$

hence

$$N_1(t) = \int \exp(-\beta A_{10} t) + \xi \exp(-(A_{21} + 4B_{12}\overline{W})t) \qquad (92).$$

However, since $(A_{21} + 4B_{12}\overline{W}) \simeq 10^8$ sec^{-1} the second term in the above expression for $N_1(t)$ rapidly goes to zero and $N_1(t)$ can be written as

$$N_1(t) \simeq N_1(0) \exp(-\beta A_{10} t) \qquad (93),$$

where $N_1(0)$ is the population of the ^3P system at time,

t = 0. One should note that this equation is identical to equation (30) for the time dependence of the population of the ^3P levels. In deriving equation (30) the absorption of light by atoms in the ^3P levels was not taken into account. It may therefore be concluded that the population of the ^3P system was not changed by the process of absorption of radiation by atoms in the ^3P system. These arguments may readily be extended to deal with the case where atoms are being excited from the ^3P level to many higher excited levels as in the Ca experiment. It could be shown that once again no appreciable alteration of the ^3P population occurs.

Finally, the total intensity of the Ca lamp was measured to establish that there would never be a significant population of atoms in excited levels other than the ^3P levels. From these measurements it can be concluded that if all the Ca discharge lamp light was absorbed by atoms in the ^3P levels only 0.001% of the ^3P population would be in higher excited levels.

APPENDIX II

The lifetime of the $^3P_1$ level in Ca and Mg was measured by monitoring the absorption of light by atoms in the $^3P_2$, $^3P_1$ or $^3P_0$ levels as a function of time. In the Ca experiment the voltage output of a spectrophotometer was sampled by the Analog-to-Digital Converter of the PDP-LAB8/E computer every 0.05 msec in order to monitor this absorption. In the Mg experiment the absorption signal was sampled every 0.5 msec. Two hundred data points were acquired from each absorption signal. A program was written in Basic R/T and used by the mini-computer to analyze the data. This program is listed in Table 18.

In the first group of statements, which are numbered from 10 to 166, the computer is instructed to acquire and signal average absorption data. Arrays for storing and plotting the data are dimensioned and the number of signals to be averaged, N, is entered. The subroutine, UCOM A, is called to sample the absorption signals and store the voltage and time values in an array, A. The signal averaging of the N absorption signals is performed in statements 40 through 100. Statements 110 through 145 instruct the computer to calculate the D.C. baseline of the light, Q, from the mean of the last 55 data points of the signal averaged absorption signal. The next group of statements, 147 to 166, subtract Q from the signal averaged data points,

TABLE 18

DATA ACQUISITION AND ANALYSIS PROGRAM

```
10 DIM A(200),B(200),C(140)
20 USE C
21 PRINT "INPUT N"
22 INPUT N
25 FOR J=1 TO N
27 CLEAR
30 UCOM A
31 GO TO 40
32 FOR I=1 TO 100
34 PLOT I/100,(A(I)+1)/2
35 DELAY
36 NEXT I
40 FOR I=1 TO 200
50 B(I)=B(I)+A(I)
60 NEXT I
70 NEXT J
80 FOR I=1 TO 200
90 B(I)=B(I)/N
100 NEXT I
110 Q=0
120 FOR I=146 TO 200
130 Q=Q+B(I)
140 NEXT I
145 Q=Q/55
147 CLEAR
150 FOR I=1 TO 200
160 B(I)=B(I)-Q
165 PLOT I/200,(B(I)+1)/2
166 DELAY\NEXT I
172 INPUT G\IF G=1GO TO 10
180 PRINT "INPUT C3,D3,T,V"
190 INPUT C3,D3,T,V
191 INPUT S
192 C2=(B(S)+B(S+1))/2
193 D2=C2/2
194 PRINT "PLOT?(YES=1,NO=0)"\INPUT Z
195 CLEAR\P=0
205 DEF FNA(I)=C2*EXP(-(I-S)/(200*C3))
220 FOR I=S TO 100
230 V=B(I)-FNA(I)
240 P=P+V*V
250 NEXT I
260 C3=C3+D3
270 P1=0
280 FOR I=S TO 100
290 V=B(I)-FNA(I)
300 P1=P1+V*V
315 IF Z=2GO TO 340
320 PLOT I/100,(B(I)+1)/2
330 PLOT I/100,(FNA(I)+1)/2
340 DELAY\NEXT I
350 CLEAR
360 IF ABS((P1-P)/P)<TGO TO 390
370 IF P1<FGO TO 390
380 C3=C3-D3\D3=-D3/2\GO TO 260
390 C2=C2+D2
400 P2=0
410 FOR I=S TO 100
420 V=B(I)-FNA(I)
430 P2=P2+V*V
435 IF Z=2GO TO 460
440 PLOT I/100,(B(I)+1)/2
450 PLOT I/100,(FNA(I)+1)/2
460 DELAY\NEXT I\CLEAR
470 IF ABS((P2-P1)/P1)<TGO TO 900
480 IF P2<P1GO TO 600
490 C2=C2-D2\D2=-D2/2\GO TO 390
600 P=P2\GO TO 260
900 F=(ABS((P1-P)/P)>T)
910 IF F=0 THEN 1000
920 GO TO 600
1000 FOR I=1 TO 199 STEP 2
1020 PLOT I/200,(B(I)+1)/2
1030 PLOT I/200,(FNA(I)+1)/2
1040 DELAY\NEXT I
1050 PRINT C2,C3,P,P1,P2
1060 PRINT 34*C3,34*D3,1/(34*C3),(V*97.3+91)
1070 STOP
2000 CLEAR
2010 PLOT .5,0
2020 PLOT .5,.999
2030 PLOT .5,(ADC(1)+1)/2
2040 DELAY
2050 GO TO 2000
```

B(I), and plot the result of signal averaging N absorption signals from which the D.C. baseline has been subtracted.

The next major group of statements, 172 to 920, comprise the least squares search routine used to fit the data to the theoretical absorption model. The computer is first instructed to ask if the data is to be accepted or rejected. If the data is rejected, new data is acquired and signal averaged. If the data is to be analyzed, initial estimates of the observed lifetime, C3, and the stepsize by which the lifetime is to be changed, D3, are entered.

The tolerance to which the least squares fit is to be performed, T, is also entered along with the temperature, W, in millivolts (i.e., the value of the thermal emf produced in the thermocouple). Next the number of the initial data point, S, to be included in the fit is entered. Provision is made to plot each trial in the fitting process or to just plot the final fit and the signal averaged data points at the user's discretion. A fit is made to the equation

$$FNA(I) = C2 * EXP(-(I-S)/(200 * C3)) \qquad (94),$$

where C2 is the amplitude coefficient. The fit is performed using the data points from I = S to 100. The lifetime, C3, is initially estimated by minimizing the sum of the squares of the deviations of the data from the fitting function by an iterative searching routine until some preset tolerance is reached. The initial estimate for the amplitude coefficient, C2, is made by taking the average of the

voltage of the first two data points used in the fit as the value of C2. After the value of the lifetime has been estimated reasonably well, an iterative search is carried out to determine the best value of the parameter C2. The value of the lifetime is then re-estimated using this new value of C2. This procedure is continued until both parameters have been determined such that the sum of the squares of the differences between the fitting function and the signal average data is less than some preset value. Statements 1000 to 1070 cause the final fit and data to be plotted as well as the final estimates of the lifetime, C3, and the amplitude coefficient, C2, to be printed. The observed lifetime, C3, is multiplied by β to obtain the true lifetime, τ. The true lifetime, τ, as well as its reciprocal are then printed.

Statements 2000 to 2050 comprise a subroutine that may be called by typing the statement GO to 2000. This routine causes the value of the voltage incident on the Analog-to-Digital Converter channel on which the absorption signal is measured to be plotted in order that the value of the D.C. baseline may be checked.